

1 Dear Editor Hannah Cloke,

2 Thanks for your and all reviewers' recommendations. We improved the  
3 manuscript following the suggestions. The main changes are:

- 4 1. The introduction has been revised to improve the review of soil moisture and  
5 surface temperature assimilation, the background of this study, etc.
- 6 2. The order of figures has been changed, the Fig. 6, Fig. 7 and Fig. 8 have been  
7 combined and Table 3 has been deleted.
- 8 3. The discussion on bias estimation, observation error, definition of the state vector,  
9 COSMIC model and COSMOS has been extended,

10

11 **Editor comments:**

12 Thank you for your author responses. As you are aware, the reviewers have raised a  
13 number of concerns. I invite you to submit a revised manuscript which incorporates  
14 your suggested comments to address these reviewer concerns. Please take special care  
15 with the clarity of your manuscript so it is always entirely clear what you are  
16 undertaking. Where necessary this could involve a further sentence or two explaining  
17 background work/references of importance.

18 [Response: the corresponding changes have been made following the reviewer  
19 comments.](#)

20

21 **Reviewer 1:**

22 General comment: The major contribution of this work is to improve CLM  
23 performances by assimilating cosmic-ray data and LST data over irrigated site with  
24 Local Ensemble Transform Kalman Filter method. Basically, the idea is good. It is  
25 impressive to update soil moisture and temperature by jointly assimilation of  
26 cosmic-ray data and LST. Moreover, the turbulent heat fluxes are improved  
27 significantly. However, the manuscript is lacking in detail in a few areas and I'd not  
28 recommend the paper for publication unless substantial improvements are made to  
29 address the following concerns.

30 [Response: thanks for the recommendation. We handled your comments, see below.](#)

31

32 Major comments:

33 1. The introduction section needs to be carefully revised. The aim of this paper is to  
34 correct biases in CLM forcing, and improve model performances (e.g. soil  
35 moisture profile, ET) by assimilating cosmic-ray data and LST. However, the  
36 authors pay less attention on soil moisture and LST assimilation; only two  
37 sentences focus on soil moisture and temperature assimilation progresses were  
38 stated in the introduction part. The progresses should be enhanced in this part.  
39 Moreover, on page 9031, “In CLM, the surface fluxes are calculated based on the  
40 Monin–Obukhov similarity theory. The sensible heat flux is formulated as a  
41 function of temperature and leaf area index, and the latent heat flux is formulated  
42 as a function of the temperature and leaf stomatal resistances. The leaf stomatal  
43 resistance is calculated from the Ball-Berry conductance model (Collatz et al.,  
44 1991). The surface fluxes are therefore sensitive to the surface and soil  
45 temperature.” this sentence looks wired, why surface fluxes are sensitive to soil  
46 temperature, the previous sentences cannot lead to this conclusion. Then why  
47 calibrate LAI? It is stated abrupt. Any other persons focus on LAI calibration to  
48 improve ET? I recommend authors rewrite the introduction part to describe more  
49 logically.

50 **Response:** We improved the introduction in the revision for the soil moisture and  
51 LST assimilation. (line 116-134)

52 “The positive impact of soil moisture data assimilation was shown in several  
53 studies. Importantly, surface soil moisture could be used to obtain better  
54 characterization of the root zone soil moisture (Barrett and Renzullo, 2009; Crow  
55 et al., 2008; Das et al., 2008; Draper et al., 2011; Li et al., 2010). It was also  
56 shown that the assimilation of soil moisture observations can be used to correct  
57 rainfall errors (Crow et al., 2011; Yang et al., 2009). Often a systematic bias  
58 between measured and modelled soil moisture content can be found; soil moisture  
59 estimation can be significantly improved using joint state and bias estimation (De  
60 Lannoy et al., 2007; Kumar et al., 2012; Reichle et al., 2008). Also studies on data

61 assimilation of remotely sensed land surface temperature products show a positive  
 62 impact on the estimation of soil moisture, latent heat flux and sensible heat flux  
 63 (Ghent et al., 2010; Xu et al., 2011). Also in these studies it was found that bias, in  
 64 these cases soil temperature bias, of land surface models can be removed with  
 65 land surface temperature assimilation (Bosilovich et al., 2007; Reichle et al.,  
 66 2010). Other studies updated both land surface model states and parameters with  
 67 soil moisture and land surface temperature data (Bateni and Entekhabi, 2012; Han  
 68 et al., 2014a; Montzka et al., 2013; Pauwels et al., 2009). The assimilation of  
 69 measured cosmic-ray neutron counts in a land surface model was successfully  
 70 tested, but these studies focused on state updating alone (Rosolem et al., 2014;  
 71 Shuttleworth et al., 2013).”

72

73 The update of soil temperature is defined as:

$$74 \quad \Delta T_{soil} = f(h)/-\lambda$$

75 where  $\lambda$  is the thermal conductivity.

76 The heat flux  $h$  into the soil surface from the overlying atmosphere is defined  
 77 as:

$$78 \quad h = \vec{S}_{soil} + \vec{L}_{soil} - H_{soil} - \lambda E_{soil}$$

79  $\vec{S}_{soil}$  is the solar radiation absorbed by top soil,  $\vec{L}_{soil}$  is the longwave  
 80 radiation absorbed by soil,  $H_{soil}$  is the sensible heat flux from soil,  $\lambda E_{soil}$  is the  
 81 latent heat flux from soil.

82 The update of vegetation temperature is defined as:

$$83 \quad \Delta T_v = \frac{\vec{S}_v - \vec{L}_v - H_v - \lambda_{vap} E_v}{\frac{\partial \vec{L}_v}{\partial T_v} + \frac{\partial \vec{H}_v}{\partial T_v} + \frac{\partial \lambda E_v}{\partial T_v}}$$

84  $\vec{S}_v$  is the solar radiation absorbed by the vegetation,  $\vec{L}_v$  is the net longwave  
 85 radiation absorbed by vegetation,  $H_v$  and  $\lambda_{vap} E_v$  are the sensible and latent  
 86 heat fluxes from vegetation.

87 The above equations show the sensitivity of vegetation temperature to the

88 surface heat fluxes. Measured land surface temperature is composed of the land  
89 surface temperature and vegetation temperature. Therefore, a mismatch of land  
90 surface temperature is statistically linked to a mismatch of land surface fluxes. On  
91 the other hand, land surface fluxes are also sensitive to soil moisture content.  
92 Therefore, land surface temperature shows a statistical correlation with soil  
93 moisture content and allows to update soil moisture content. In various papers,  
94 land surface temperature assimilation served to improve the estimation of surface  
95 fluxes (Ghent et al., 2010; Meng et al., 2009; Reichle et al., 2010; Xu et al., 2011).  
96 The relation between the soil temperature / vegetation temperature and surface  
97 fluxes has been explained in the revision. (line 162-174)

98 “In CLM, land surface fluxes are calculated based on the Monin-Obukhov  
99 similarity theory. The sensible heat flux is formulated as a function of  
100 temperature and LAI, and the latent heat flux is formulated as a function of the  
101 temperature and leaf stomatal resistances. The leaf stomatal resistance is  
102 calculated from the Ball-Berry conductance model (Collatz et al., 1991). The  
103 updates of soil temperature and vegetation temperature are derived based on the  
104 solar radiation absorbed by top soil (or vegetation), longwave radiation absorbed  
105 by soil (or vegetation), sensible heat flux from soil (or vegetation) and latent heat  
106 flux from soil (or vegetation). Measured land surface temperature is composed of  
107 the ground temperature and vegetation temperature. Therefore a difference  
108 between measured and calculated land surface temperature can be adjusted by  
109 changing land surface fluxes. As land surface fluxes are sensitive to soil moisture  
110 content, land surface temperature is sensitive to soil moisture content.”

- 111 1) Ghent, D., Kaduk, J., Remedios, J., Ardo, J., and Balzter, H.: Assimilation of  
112 land surface temperature into the land surface model JULES with an  
113 ensemble Kalman filter, *J Geophys Res-Atmos*, 115, 2010.
- 114 2) Meng, C. L., Li, Z. L., Zhan, X., Shi, J. C., and Liu, C. Y.: Land surface  
115 temperature data assimilation and its impact on evapotranspiration estimates  
116 from the Common Land Model, *Water Resour Res*, 45, 2009.
- 117 3) Reichle, R. H., Kumar, S. V., Mahanama, S. P. P., Koster, R. D., and Liu, Q.:

118 Assimilation of Satellite-Derived Skin Temperature Observations into Land  
119 Surface Models, *J Hydrometeorol*, 11, 1103-1122, 2010.

120 4) Xu, T. R., Liu, S. M., Liang, S. L., and Qin, J.: Improving Predictions of  
121 Water and Heat Fluxes by Assimilating MODIS Land Surface Temperature  
122 Products into the Common Land Model, *J Hydrometeorol*, 12, 227-244,  
123 2011.

124 Our study was also based on the conclusions of Schwinger, J., et al., 2010:  
125 “results confirm that soil texture and LAI are key parameters that have a  
126 dominant influence on modeled LE under specific environmental conditions in  
127 CLM4.” More works have studied the sensitivity of land surface models to the  
128 leaf area index (Ghilain et al., 2012; Jarlan et al., 2008; Schwinger et al., 2010;  
129 van den Hurk et al., 2003; Yang et al., 1999). Moreover, we used the MODIS  
130 LAI in CLM, whereas the MODIS products usually underestimate the LAI  
131 compared with field measurements, as was found in validation studies by the  
132 NASA (<http://landval.gsfc.nasa.gov>): the underestimation by the MODIS LAI  
133 product is  $0.66 * \text{LAI (MODIS)}$  for all biomes and  $0.5 * \text{LAI (MODIS)}$  except for  
134 broadleaf forests. We improved the introduction in the revision. (line 180-188)

135 “Soil moisture, land surface temperature and LAI influence the estimation of  
136 latent and sensible heat fluxes (e.g., Ghilain et al., 2012; Jarlan et al., 2008;  
137 Schwinger et al., 2010; van den Hurk et al., 2003; Yang et al., 1999), and  
138 therefore this study focuses in addition on the calibration of LAI with help of the  
139 assimilation of land surface temperature. However, there are large discrepancies  
140 between the remotely retrieved LAI and measured values, and the MODIS LAI  
141 product underestimates in situ measured LAI by 44% on average  
142 (<http://landval.gsfc.nasa.gov/>), and therefore the LAI is also calibrated by data  
143 assimilation.”

144 1) Schwinger, J., et al. "Sensitivity of Latent Heat Fluxes to Initial Values and  
145 Parameters of a Land-Surface Model." *Vadose Zone Journal* **9**(4): 984-1001,  
146 2010.

147 2) Ghilain, N., Arboleda, A., Sepulcre-Canto, G., Batelaan, O., Ardo, J., and

148 Gellens-Meulenberghs, F.: Improving evapotranspiration in a land surface  
149 model using biophysical variables derived from MSG/SEVIRI satellite,  
150 Hydrology and Earth System Sciences, 16, 2567-2583, 2012.

151 3) Jarlan, L., Balsamo, G., Lafont, S., Beljaars, A., Calvet, J. C., and Mougin, E.:  
152 Analysis of leaf area index in the ECMWF land surface model and impact on  
153 latent heat and carbon fluxes: Application to West Africa, J Geophys  
154 Res-Atmos, 113, 2008.

155 4) Schwinger, J., Kollet, S. J., Hoppe, C. M., and Elbern, H.: Sensitivity of  
156 Latent Heat Fluxes to Initial Values and Parameters of a Land-Surface Model,  
157 Vadose Zone J, 9, 984-1001, 2010.

158 5) van den Hurk, B. J. J. M., Viterbo, P., and Los, S. O.: Impact of leaf area  
159 index seasonality on the annual land surface evaporation in a global  
160 circulation model, J Geophys Res-Atmos, 108, 2003.

161 6) Yang, Z. L., Dai, Y., Dickinson, R. E., and Shuttleworth, W. J.: Sensitivity of  
162 ground heat flux to vegetation cover fraction and leaf area index, J Geophys  
163 Res-Atmos, 104, 19505-19514, 1999.

164

165 2. In section 3, LAI was updated by assimilating LST and soil moisture, I'm not  
166 certain if it is correct to do this. Does LST and soil moisture are strong correlated  
167 to LAI? Please state their relationship clearly.

168 Response: the LST was used to update the LAI, not soil moisture or Cosmic-ray.  
169 This has been clarified in the revision (line 183-184). Details can be found in our  
170 response to question 1. The introduction in the revision has been improved.

171

172 3. In this study, the soil moisture related instrument, the cosmic-ray, is a ground  
173 measurement instrument. It can be used to measure soil moisture at plot scale  
174 about 600 m. it is hard and expensive to be applied at the continent scales.  
175 However, MODIS LST can be easily obtained globally. Thus, the limitation of  
176 assimilating cosmic-ray data should be discussed.

177 Response: the Cosmic-ray Soil Moisture Observing System (COSMOS) has been

178 designed as a continental scale network by installing 500 COSMOS probes across  
179 the USA (Zreda et al., 2012). Nevertheless, it is true that there are still some  
180 disadvantages of COSMOS compared with remote sensing. COSMOS is also  
181 expensive for extensive deployment to measure the continental/regional scale soil  
182 moisture. This discussion has been added in the revision. (line 642-647)

183 “Although the Cosmic-ray Soil Moisture Observing System (COSMOS) has been  
184 designed as a continental scale network by installing 500 COSMOS probes across  
185 the USA (Zreda et al., 2012), there are still some disadvantages of COSMOS  
186 compared with remote sensing. COSMOS is also expensive for extensive  
187 deployment to measure the continental/regional scale soil moisture.”

188 1) Zreda, M., Shuttleworth, W. J., Zeng, X., Zweck, C., Desilets, D., Franz, T.  
189 E., and Rosolem, R.: COSMOS: the COsmic-ray Soil Moisture Observing  
190 System, *Hydrology and Earth System Sciences*, 16, 4079-4099, 2012.

191

192 Minor comments

193 1. On page 9040, the augmentation method was used to update surface temperature,  
194 ground temperature, vegetation temperature and 10 layers of soil temperature by  
195 assimilating LST. However, surface temperature and vegetation temperature are  
196 diagnostic variables in CLM. To change them at the current time step may not  
197 influence model estimates in next time step. It is wasting time to add them as the  
198 updated variables. Remove them in the vectors.

199 Response: Thanks for the suggestion. CLM needs the initial state of the ground  
200 temperature, vegetation temperature and 15 layers of soil temperature. For  
201 example, the calculation of vegetation temperature in CLM is:  $T_v^{n+1} = T_v^n + \Delta T_v$ .  
202 Only the surface temperature is the diagnostic variable. Because we calculated  
203 the surface temperature with help of an observation operator for assimilation  
204 purpose only, it is the right state to be assimilated. In order to calculate the  
205 Kalman gain, we need the surface temperature to compare with the MODIS LST.  
206 For reasons of technical simplicity, we calculated the surface temperature out of  
207 Kalman filter and transferred the calculated surface temperature into Kalman

208 filter through the state vector. It means the identity matrix was used as the  
209 observation operator  $H$  in the Kalman filter.

210

211 2. In section 2.2, please state what meteorology parameters are used as the forcing  
212 data in CLM, and how long is the time step of CLM run?

213 Response: The incident longwave radiation, incident solar radiation, precipitation,  
214 air pressure, specific humidity, air temperature and wind speed were used in  
215 CLM. The time step of CLM was hourly. (line 238-240)

216

217 3. The forcing data were perturbed by set of noises, what are the observation errors  
218 of cosmic-ray data and MODIS LST? How to perturb them?

219 Response: The observation data were not perturbed in LETKF because it is a  
220 square root Kalman filter. Only the classical ensemble Kalman filter (EnKF)  
221 needs to perturb the observations. The variance of Cosmic-ray was the measured  
222 neutron count value (Zreda, M., et al., 2012) and the variance of MODIS LST  
223 was assumed to be 1 K (Wan, Z. and Z. L. Li, 2008), and the error of MODIS  
224 LST has been verified (<http://landval.gsfc.nasa.gov>) by many studies. (line  
225 460-464)

226 “The variance of the instantaneous measured neutron intensity is equal to the  
227 measured neutron count intensity (Zreda et al., 2012) and smaller for temporal  
228 averaging for daily or sub-daily applications. The instantaneous neutron intensity  
229 was assimilated in this study. The variance of MODIS LST was assumed to be 1  
230 K (Wan and Li, 2008)”

231

232 1) Zreda, M., et al. (2012). "COSMOS: the COsmic-ray Soil Moisture  
233 Observing System." Hydrology and Earth System Sciences 16(11):  
234 4079-4099.

235 2) Wan, Z. and Z. L. Li (2008). "Radiance - based validation of the V5 MODIS  
236 land - surface temperature product." International Journal of Remote Sensing  
237 29(17-18): 5373-5395.



238

239 4. The caption of figure 4 can be change as "Same as figure 3 but for 50 cm and 80  
240 cm"

241 [Response: thanks, changed.](#)

242

243 5. The figures 6, 7, and 8 can be combined into one figure, as they are all turbulent  
244 heat fluxes.

245 [Response: thanks, changed.](#)

246

247 6. The ignorance of energy imbalance problem for eddy covariance system may  
248 cause some error in producing ET observation. This should be discussed.

249 [Response: the discussion has been added in the revision. \(line 526-528\)](#)

250 "The true evapotranspiration is therefore likely larger, but not much larger as the  
251 energy balance gap was limited (3.7%)."

252

253

254 **Reviewer 2:**

255 General comments

256 The paper provides an important contribution to the research on data assimilation in  
257 land surface modelling. The paper considers assimilation of cosmic-ray soil moisture  
258 data and land surface temperature in the Community Land Model (CLM).  
259 Assimilation of the data sources individually and jointly as well as in combination  
260 with estimation of leaf area index are evaluated with respect to soil moisture,  
261 evapotranspiration, and latent and sensible heat flux. The paper is, in general, well  
262 written and technically sound. However, some elaborations are needed; especially on  
263 the Kalman filter setup and evaluation (see detailed comments below).

264 [Response: Thanks for your recommendation. We have improved the manuscript  
265 according to the responses below.](#)

266

267 Detailed comments

268 1. Page 9031, line 10-13. Not clear. Inclusion of bias in the Kalman filter is usually  
269 defined either as a bias in the system equation or a bias in the observation  
270 equation. The specific source of error need not be known.

271 Response: Before we estimate the bias, we should determine whether the bias  
272 comes from the model, observation, or both. If the source of bias is not attributed  
273 to the right source, model predictions cannot be improved. In the Kalman filter  
274 equation, the model bias and the observation bias are handled differently: the  
275 model bias is removed in the model forecast  $x^b = x^b - bias_{model}$ ; the  
276 observation bias is removed from the innovation part  $K \times (y_{obs} - bias_{obs} - x^b)$ .  
277 In summary, the source of the bias should be defined before estimation. A  
278 comprehensive overview of bias estimation is given by Dee (2005). According to  
279 the description, “By design, bias-aware assimilation requires assumptions about  
280 the nature of the biases: first, the attribution of a bias to a particular source, and  
281 second, a characterization of the bias in terms of some well-defined set of  
282 parameters”. In this paper, no explicit model for observation bias or model bias  
283 was assumed, and no explicit bias estimation was done for simplicity.  
284 Nevertheless, the model states were corrected by the observations. We have  
285 clarified this part in the revision. (line 154-160)

286 “The bias can be attributed to the model structure, model parameters, atmospheric  
287 forcing or observation data, and the bias-aware assimilation requires the  
288 assumption that the bias comes from a particular source. If the source of bias is  
289 not attributed to the right source, model predictions cannot be improved (Dee,  
290 2005). Therefore bias-blind assimilation in which the bias estimation was not  
291 handled explicitly was used for safety. Instead, it was investigated whether  
292 neutron counts measured by cosmic-ray probe were able to correct for the bias.”

293

294 1) Dee, D. P. (2005). "Bias and data assimilation." Quarterly Journal of the  
295 Royal Meteorological Society **131**(613): 3323-3343.

296

297 2. Page 9031, line 13. Not clear what is meant by ‘bias blind assimilation’ and why

298 this is applied for ‘safety’.

299 Response: The bias blind assimilation is the traditional data assimilation without  
300 bias estimation. Dee et al. (2005) wrote: “If the source of a known bias is  
301 uncertain, bias-blind assimilation may be the safest option. The main scientific  
302 challenge is to correctly attribute a detected bias to its source, and then to develop  
303 a useful model for the bias. When different sources produce similar biases, the  
304 assimilation may correct the wrong source.” Because the study area is a very  
305 heterogeneous irrigated farmland, both the observation and model could be biased.  
306 In CLM, the main bias came from the atmospheric forcing input due to the lack of  
307 irrigated water amount, but the bias could also come from wrong soil properties  
308 (e.g. sand fraction, clay fraction and organic matter density) and other vegetation  
309 parameters (e.g. leaf area index,  $V_{cmax}$ ). For example, three papers studied the  
310 sensitivity of the latent heat flux and sensible heat flux to the hydraulic parameters  
311 (Hou, et al., 2012) and vegetation parameters  $V_{cmax}$  (Bonan, et al., 2011) in  
312 CLM4, and soil moisture and leaf area index (Schwinger, et al., 2010) in CLM4.  
313 In each of these studies, the assumption was made that the other sensitive  
314 parameters were defined properly. In this study, we focused on the model bias  
315 introduced by the forcing data and the leaf area index, and neglected the other  
316 sources of bias. We have clarified the discussion in the revision. (see response to  
317 earlier reviewer question)

318

- 319 1) Hou, Z. S., et al. (2012). "Sensitivity of surface flux simulations to hydrologic  
320 parameters based on an uncertainty quantification framework applied to the  
321 Community Land Model." *Journal of Geophysical Research-Atmospheres*  
322 117.
- 323 2) Bonan, G. B., et al. (2011). "Improving canopy processes in the Community  
324 Land Model version 4 (CLM4) using global flux fields empirically inferred  
325 from FLUXNET data." *Journal of Geophysical Research-Biogeosciences* 116.
- 326 3) Schwinger, J., et al. (2010). "Sensitivity of Latent Heat Fluxes to Initial  
327 Values and Parameters of a Land-Surface Model." *Vadose Zone Journal* 9(4):

328 984-1001.

329

330 3. Page 9031, line 17. Define 'CLM'.

331 Response: CLM is Community Land Model, was included in the revision.

332

333 4. Page 9036, line 8-10. Are the measured data at the station in Switzerland  
334 representative for the Chinese case study?

335 Response: The data are used to remove temporal (secular or diurnal) variations  
336 caused by the sunspot cycle. We follow the standard approach applied by the  
337 COSMOS network globally, discussed in detail by Zreda et al. (2012). This  
338 reference is appropriately mentioned in the revision. (line 302-303)

339 "The temporal (secular or diurnal) variations caused by the sunspot cycle could be  
340 removed after this correction (Zreda et al., 2012)."

341

342 1) Zreda, M., et al. (2012). "COSMOS: the COsmic-ray Soil Moisture  
343 Observing System." Hydrology and Earth System Sciences 16(11):  
344 4079-4099.

345

346 5. Page 9036, line 24-26. Soil moisture from 10 soil layers (does this correspond to  
347 the top 10 cm of the soil?) in CLM is used as input to COSMIC. The effective  
348 measurement depth of the cosmic-ray probe depends on soil moisture, so why is a  
349 fixed depth used here? I expect this will introduce a bias in the simulated soil  
350 moisture for comparison with the measurements.

351 Response: The thickness of top 10 soil layers in CLM is about 3.8 m. Because the  
352 effective measurement depth of cosmic-ray probe is between 12 and 76 cm, it is  
353 unlikely that anything beyond 1 m deep will substantially impact the results. The  
354 COSMIC model assumes a more detailed soil profile. In COSMIC, the soil  
355 moisture information from the 10 layers from CLM was interpolated to  
356 information for 300 layers based on the soil layer depth for stable numerical  
357 solution. The contribution of each soil layer to the measured neutron flux changes

358 temporally depending on the soil moisture condition. Therefore the effective  
359 measurement depth of the cosmic ray probe also changes temporally. The  
360 explanation in the manuscript was improved. (line 317-328)

361 “The simulated soil moisture content for 10 CLM soil layers (3.8 m depth) was  
362 used as input to COSMIC in order to simulate the corresponding neutron count  
363 intensity and compare it with the measured neutron count intensity. It should be  
364 mentioned that it is unlikely that anything beyond 1 m deep will substantially  
365 impact the results because the effective measurement depth of the cosmic-ray  
366 probe is between 12 and 76 cm. The COSMIC model assumes a more detailed soil  
367 profile. COSMIC interpolates the soil moisture information from the ten CLM soil  
368 layers to information for 300 soil layers of depth 1cm. The contribution of each  
369 soil layer to the measured neutron flux will change temporally depending on the  
370 soil moisture condition. Therefore the effective measurement depth of the cosmic  
371 ray probe will also change temporally. COSMIC calculates the vertically weighted  
372 soil moisture content based on the vertical distribution of soil moisture content.”

373

374 6. Page 9039, line 1. Definition of state vector not clear. Why soil moisture from 10  
375 layers (see previous comment) and soil temperature for 15 layers?

376 Response: These are the standard CLM layout for soil moisture and soil  
377 temperature. The hydrology calculations are done over the top 10 layers, and the  
378 bottom 5 layers are specified as bedrock. The lower 5 layers are hydrologically  
379 inactive layers. Temperature calculations are done over all layers. The manuscript  
380 has been revised to include this explanation. (line 422-426)

381 “The 10 layers of soil moisture and 15 layers of soil temperature are the standard  
382 CLM layout for both soil moisture and soil temperature. The hydrology  
383 calculations are done over the top 10 layers, and the bottom 5 layers are specified  
384 as bedrock. The lower 5 layers are hydrologically inactive layers. Temperature  
385 calculations are done over all layers (Oleson et al., 2013)”

386

387 7. Page 9040, line 17-20. How is the leaf area index represented in the augmented

388 system equation? As a persistence model?

389 Response: the leaf area index was treated as a parameter and updated with help of  
390 the augmented state vector approach, but only changed after each update. For the  
391 calibration of the LAI, the state vector was augmented with surface temperature,  
392 ground temperature, vegetation temperature, soil temperature for 15 layers and  
393 LAI if only the land surface temperature observations were assimilated without  
394 soil moisture update. This resulted then in a state dimension of 19. (line 380-384)  
395 “For the calibration of the LAI, the state vector was augmented with surface  
396 temperature, ground temperature, vegetation temperature, soil temperature for 15  
397 CLM-layers and LAI if only the land surface temperature observations were  
398 assimilated without soil moisture update. This resulted then in a state dimension  
399 of 19.”

400

401 8. Page 9041, line 1-15. The Kalman filter settings are not sufficiently discussed.  
402 They seem rather arbitrarily chosen. It is not clear how the standard deviations,  
403 spatial and temporal correlations, and cross correlations given in Table 1 are  
404 determined. Has sensitivity analysis been applied to analyse the sensitivity of  
405 ensemble size and model error statistics on the assimilation results? You can  
406 analyse the prediction uncertainty provided by the Kalman filter to evaluate the  
407 Kalman filter settings by comparing measurements with predicted confidence  
408 bands or analyse the statistical properties of the model innovations. Definition of  
409 measurement uncertainty is not described.

410 Response: the values of standard deviations and temporal correlations in Table I  
411 were chosen based on commonly used values in previous catchment scale and  
412 regional scale data assimilation studies (Kumar et al., 2009; Reichle et al., 2010;  
413 De Lannoy et al., 2012). In the 3D-EnKF, the imposed spatial correlation on  
414 forcing data is very important for the assimilation (Reichle and Koster, 2003; De  
415 Lannoy et al., 2009). In 1D-EnKF and LETKF (which we used), no horizontal  
416 correlation among model grid cells is calculated, so the imposed spatial  
417 correlation of forcing data will not influence the assimilation. The impacts of

418 horizontal spatial correlation on the assimilation can be included through the  
419 localization technique (Reichle and Koster, 2003; De Lannoy, et al., 2009). The  
420 selection of the ensemble size was based on the results of Han et al., 2014, who  
421 reported that for more than 30~40 ensemble members, the assimilation results  
422 could not be improved too much. Therefore 50 ensemble members were used in  
423 this study. (line 443-446)

424 “The values of standard deviations and temporal correlations in Table 1 were  
425 chosen based on previous catchment scale and regional scale data assimilation  
426 studies (De Lannoy et al., 2012; Kumar et al., 2012; Reichle et al., 2010).”

427 The observation standard deviation of cosmic-ray probes is equal to the square  
428 root of the measured neutron counts (Zreda, et al., 2012) and the observation  
429 standard deviation of MODIS land surface temperature was here equal to 1 K  
430 (Wan and Li, 2008). We added this information in the revised version of the  
431 manuscript. (line 460-464)

432 “The variance of the instantaneous measured neutron intensity is equal to the  
433 measured neutron count intensity (Zreda et al., 2012) and smaller for temporal  
434 averaging for daily or sub-daily applications. The instantaneous neutron intensity  
435 was assimilated in this study. The variance of MODIS LST was assumed to be 1  
436 K (Wan and Li, 2008)”

437

438 1) Kumar, S. V., et al. (2009). "Role of Subsurface Physics in the Assimilation  
439 of Surface Soil Moisture Observations." *Journal of Hydrometeorology* **10**(6):  
440 1534-1547.

441 2) Reichle, R. H., et al. (2010). "Assimilation of Satellite-Derived Skin  
442 Temperature Observations into Land Surface Models." *Journal of*  
443 *Hydrometeorology* **11**(5): 1103-1122.

444 3) De Lannoy, G. J. M., et al. (2012). "Multiscale assimilation of Advanced  
445 Microwave Scanning Radiometer-EOS snow water equivalent and Moderate  
446 Resolution Imaging Spectroradiometer snow cover fraction observations in  
447 northern Colorado." *Water Resources Research* **48**.

- 448 4) Reichle, R. H. and R. D. Koster (2003). "Assessing the impact of horizontal  
449 error correlations in background fields on soil moisture estimation." Journal  
450 of Hydrometeorology 4(6): 1229-1242.
- 451 5) De Lannoy, G. J. M., et al. (2009). "Satellite-Scale Snow Water Equivalent  
452 Assimilation into a High-Resolution Land Surface Model." Journal of  
453 Hydrometeorology 11(2): 352-369.
- 454 6) Han, X., et al. (2014). "Soil moisture and soil properties estimation in the  
455 Community Land Model with synthetic brightness temperature observations."  
456 Water Resources Research 50(7): 6081-6105.
- 457 7) Wan, Z. and Z. L. Li (2008). "Radiance - based validation of the V5 MODIS  
458 land - surface temperature product." International Journal of Remote Sensing  
459 29(17-18): 5373-5395.
- 460 8) Zreda, M., et al. (2012). "COSMOS: the COsmic-ray Soil Moisture  
461 Observing System." Hydrology and Earth System Sciences 16(11):  
462 4079-4099.

463

464 9. Page 9043, line 4. How is measured soil moisture estimated?

465 Response: the soil moisture for the CRS footprint scale was calculated from the  
466 arithmetic mean of the 23 SoilNet soil moisture observations. This information  
467 has been included in the manuscript. (line 304-305)

468 "In this study, the soil moisture for the CRS footprint scale was calculated from  
469 the arithmetic mean of the 23 SoilNet soil moisture observations."

470

471 10. Page 9045, line 4. Same information shown in Figs. 6-8 and Table 3. All results  
472 can be included in the table and figures omitted.

473 Response: thanks for the suggestion. Table 3 was removed in the revision.

474

475 11. Page 9045, line 3-25. It is stated that the results for latent and sensible heat flux  
476 correspond to the results obtained for soil moisture. However, there are some  
477 notable differences that should be elaborated. The effect of inclusion of parameter



478 estimation of LAI on latent and sensible heat flux depends on the type of data  
479 being assimilated. For LST assimilation an increase in RMSE is obtained when  
480 LAI estimation is included. With assimilation of both LST and CRS lower RMSE  
481 is obtained with LAI estimation. In addition, assimilation of LST provides better  
482 results than assimilation of both LST and CRS.

483 Response: thanks, in the scenario of only LST assimilation without LAI update,  
484 the latent heat flux could not be improved. The univariate assimilation of LST did  
485 not give any improvement for this case. The joint soil moisture and LAI update  
486 scenario of LST\_Feedback\_Par\_LAI was worse than the single soil moisture  
487 update scenario of LST\_Feedback in this case. This part has been improved in the  
488 discussion section of the revision. (line 509-514)

489 “Without assimilation of cosmic-ray probe neutron counts, the soil moisture  
490 simulation cannot be improved (scenario Only\_LST). However, the scenarios of  
491 LST\_Feedback and LST\_Feedback\_Par\_LAI improve the soil moisture profile  
492 characterization, which shows that explicitly using LST to update soil moisture  
493 content in the data assimilation routine gives better results than using LST only to  
494 update soil moisture by the model equations.”

495 “The scenario where soil moisture and LAI are jointly updated  
496 (LST\_Feedback\_Par\_LAI) gave worse results than the scenario of  
497 LST\_Feedback.”

498

499 12. Figure 5. Explain numbers in lower-right corner in figure caption.

500 Response: these are the accumulated ET amounts during the study period; this has  
501 been corrected in this revision. (line 523-524)

502

503

504 **Correction of Systematic Model Forcing Bias of CLM using**  
505 **Assimilation of Cosmic-Ray Neutrons and Land Surface**  
506 **Temperature: a study in the Heihe Catchment, China**

507  
508 Xujun Han<sup>1,2,3</sup>

- 509 1. Cold and Arid Regions Environmental and Engineering Research Institute,  
510 Chinese Academy of Sciences, Lanzhou, Gansu 730000, PR China  
511 2. Forschungszentrum Jülich, Agrosphere (IBG 3), Leo-Brandt-Strasse, 52425 Jülich,  
512 Germany  
513 3. Centre for High-Performance Scientific Computing in Terrestrial Systems: HPSC  
514 TerrSys, Geoverbund ABC/J, Leo-Brandt-Strasse, 52425 Jülich, Germany

515  
516 Harrie-Jan Hendricks Franssen<sup>1,2</sup>

- 517 1. Forschungszentrum Jülich, Agrosphere (IBG 3), Leo-Brandt-Strasse, 52425 Jülich,  
518 Germany  
519 2. Centre for High-Performance Scientific Computing in Terrestrial Systems: HPSC  
520 TerrSys, Geoverbund ABC/J, Leo-Brandt-Strasse, 52425 Jülich, Germany

521  
522 Rafael Rosolem

523 Department of Civil Engineering, University of Bristol, Bristol BS8 1TR, UK

524  
525 Rui Jin

526 Cold and Arid Regions Environmental and Engineering Research Institute, Chinese  
527 Academy of Sciences, Lanzhou, Gansu 730000, PR China

528  
529 Xin Li

530 Cold and Arid Regions Environmental and Engineering Research Institute, Chinese  
531 Academy of Sciences, Lanzhou, Gansu 730000, PR China

532  
533 Harry Vereecken<sup>1,2</sup>

- 534 1. Forschungszentrum Jülich, Agrosphere (IBG 3), Leo-Brandt-Strasse, 52425 Jülich,  
535 Germany  
536 2. Centre for High-Performance Scientific Computing in Terrestrial Systems: HPSC  
537 TerrSys, Geoverbund ABC/J, Leo-Brandt-Strasse, 52425 Jülich, Germany

538  
539  
540  
541  
542 Corresponding author: Xujun Han, Cold and Arid Regions Environmental and  
543 Engineering Research Institute, Chinese Academy of Sciences, Lanzhou, Gansu  
544 730000, PR China. (hanxj@lzb.ac.cn)

545

546 **Abstract**

547 The recent development of the non-invasive cosmic-ray soil moisture sensing  
548 technique fills the gap between point scale soil moisture measurements and regional  
549 scale soil moisture measurements by remote sensing. A cosmic-ray probe measures  
550 soil moisture for a footprint with a diameter of ~600 m (at sea level) and with an  
551 effective measurement depth between 12 cm to 76 cm, depending on the soil humidity.  
552 In this study, it was tested whether neutron counts also allow to correct for a  
553 systematic error in the model forcings. Lack of water management data often cause  
554 systematic input errors to land surface models. Here, the assimilation procedure was  
555 tested for an irrigated corn field (Heihe Watershed Allied Telemetry Experimental  
556 Research - HiWATER, 2012) where no irrigation data were available as model input  
557 although [for](#) the area a significant amount of water was irrigated. [In the study, the](#)  
558 [M](#)measured cosmic-ray neutron counts and Moderate Resolution Imaging  
559 Spectroradiometer (MODIS) land surface temperature (LST) products were jointly  
560 assimilated into the Community Land Model (CLM) with the Local Ensemble  
561 Transform Kalman Filter. Different data assimilation scenarios were evaluated, with  
562 assimilation of LST and/or cosmic-ray neutron counts, and possibly parameter  
563 estimation of leaf area index (LAI). The results show that the direct assimilation of  
564 cosmic-ray neutron counts can improve the soil moisture and evapotranspiration (ET)  
565 estimation significantly, correcting for lack of information on irrigation amounts. The  
566 joint assimilation of neutron counts and LST could improve further the ET estimation,  
567 but the information content of neutron counts exceeded the one of LST. Additional

568 improvement was achieved by calibrating LAI, which after calibration was also closer  
569 to independent field measurements. It was concluded that assimilation of neutron  
570 counts was useful for ET and soil moisture estimation even if the model has a  
571 systematic bias like neglecting irrigation. However, also the assimilation of LST  
572 helped to correct the systematic model bias introduced by neglecting irrigation and  
573 LST could be used to update soil moisture with state augmentation.

574 **Keywords:** Cosmic-ray neutron counts, Land surface temperature, Evapotranspiration,  
575 Land data assimilation, Parameter estimation

## 576 **1. Introduction**

577 Soil moisture plays a key role for crop and plant growth, water resources  
578 management and land surface-atmosphere interaction. Therefore accurate soil  
579 moisture retrieval is important. Point scale measurements can be obtained by methods  
580 like time domain reflectometry (TDR) (Robinson et al., 2003) and larger scale, coarse  
581 soil moisture information from remote sensing sensors (Entekhabi et al., 2010; Kerr et  
582 al., 2010). Wireless Sensor Networks (WSN) allow characterization of soil moisture at  
583 the catchment scale with many local connected sensors at separated locations (Bogena  
584 et al., 2010). TDR only measures the point scale soil moisture and the maintenance of  
585 WSN is expensive. Recently, neutron count intensity measured by above-ground  
586 cosmic-ray probes was proposed as alternative information source on soil moisture.  
587 Neutron count intensity is measured non-invasively at an intermediate scale between  
588 the point scale and the coarse remote sensing scale (Zreda et al., 2008). A network of  
589 cosmic-ray sensors (CRS) has been set-up over N-America (Zreda et al., 2012).

590 Cosmic rays are composed of primary protons mainly. The fast neutrons  
591 generated by high-energy neutrons colliding with nuclei lead to “evaporation” of fast  
592 neutrons and the generated and moderated neutrons in the ground can diffuse back  
593 into the air where their intensity can be measured by the cosmic-ray soil moisture  
594 probe. Soil moisture affects the rate of moderation of fast neutrons, and controls the  
595 neutron concentration and the emission of neutrons into the air. Dry soils have low  
596 moderating power and are highly emissive; wet soils have high moderating power and  
597 are less emissive. The neutrons are mainly moderated by the hydrogen atoms

598 contained in the soil water and emitted to the atmosphere where the neutrons mix  
599 instantaneously at a scale of hundreds of meters. The measurement area of a  
600 cosmic-ray soil moisture probe represents a circle with a diameter of ~600 m at sea  
601 level (Desilets and Zreda, 2013) and the measurement depth decreases non-linearly  
602 from ~76 cm (dry soils) to ~12 cm (saturated soils) (Zreda et al., 2008). The measured  
603 cosmic-ray neutron counts show an inverse correlation with soil moisture content. The  
604 cosmic-ray neutron intensity could be reduced to 60% of surface cosmic-ray neutron  
605 intensity if the soil moisture was increased from zero to 40% (Zreda et al., 2008). The  
606 soil moisture estimation on the basis of cosmic-ray probe based neutron counts over a  
607 horizontal footprint of hectometers received considerable attention in scientific  
608 literature during the last years (Desilets et al., 2010; Zreda et al., 2008; Zreda et al.,  
609 2012).

610 Hydrogen atoms are present as water in the soil, lattice soil water, below ground  
611 biomass, atmospheric water vapor, snow water, above ground biomass, intercepted  
612 water by vegetation and water on the ground. These additional hydrogen sources  
613 contribute to the measured neutron intensity. The role of these additional hydrogen  
614 sources should be included in the analysis of the cosmic-ray measurements in order to  
615 isolate the main contribution from soil moisture. Formulations for handling water  
616 vapor (Rosolem et al., 2013), for lattice water and organic carbon (Franz et al., 2013)  
617 and for a litter layer present on the soil surface (Bogena et al., 2013) have been  
618 developed.

619 [It was shown that the assimilation of soil moisture observations could be used to](#)

620 correct the rainfall errors ; the soil moisture estimation can be significantly improved  
621 using the joint state and bias estimation The positive impact of soil moisture data  
622 assimilation was shown in several studies. Importantly, surface soil moisture could be  
623 used to obtain better characterization of the root zone soil moisture (~~Barrett and~~  
624 ~~Renzullo, 2009; Crow et al., 2008;~~(Barrett and Renzullo, 2009; Crow et al., 2008; Das  
625 et al., 2008; Draper et al., 2011; Li et al., 2010)~~Das et al., 2008; Draper et al., 2011;~~  
626 ~~Li et al., 2010~~). It was also shown that the assimilation of soil moisture observations  
627 can be used to correct rainfall errors (Crow et al., 2011; Yang et al., 2009)~~(Crow et al.,~~  
628 ~~2011; Yang et al., 2009)~~. Often a systematic bias between measured and modelled soil  
629 moisture content can be found; soil moisture estimation can be significantly improved  
630 using joint state and bias estimation (De Lannoy et al., 2007; Kumar et al., 2012;  
631 Reichle, 2008)~~(De Lannoy et al., 2007; Kumar et al., 2012; Reichle et al., 2008)~~. Also  
632 studies on data assimilation of remotely sensed land surface temperature products  
633 show a positive impact on the estimation of soil moisture, latent heat flux and sensible  
634 heat flux (Ghent et al., 2010; Xu et al., 2011)~~(Ghent et al., 2010; Xu et al., 2011)~~.  
635 Also in these studies it was found that bias, in these cases soil temperature bias, of  
636 land surface models can be removed with land surface temperature assimilation  
637 (Bosilovich et al., 2007; Reichle et al., 2010)~~(Bosilovich et al., 2007; Reichle et al.,~~  
638 ~~2010)~~. Other studies updated both land surface model states and parameters with soil  
639 moisture and land surface temperature data (Bateni and Entekhabi, 2012; Han et al.,  
640 2014a; Montzka et al., 2013; Pauwels et al., 2009)~~(Bateni and Entekhabi, 2012; Han~~  
641 ~~et al., 2014a; Montzka et al., 2013; Pauwels et al., 2009)~~. The assimilation of

642 measured cosmic-ray neutron counts in a land surface model was successfully tested,  
643 but these studies focused on state updating alone (Rosolem et al., 2014b; Shuttleworth  
644 et al., 2013)~~(Han et al., 2014b; Rosolem et al., 2014; Shuttleworth et al., 2013).~~; the  
645 surface soil moisture could be used to obtain better characterization of the root zone  
646 soil moisture . The studies of data soil moisture measurements are useful for  
647 improving the soil moisture profile estimation in land surface models or hydrologic  
648 models. Assimilation of remotely sensed land surface temperature products also  
649 improves the estimation of evapotranspiration~~show the positive impacts on land~~  
650 surface states estimation; the soil moisture, latent heat flux and sensible heat flux  
651 could be improved by assimilating the remote sensed land surface temperature ; the  
652 soil temperature bias of land surface model could be removed using the land surface  
653 temperature assimilation . The joint state and parameter estimation in land surface  
654 model with soil moisture and land surface temperature also shows the success . The  
655 assimilation of measured cosmic ray neutron counts in a land surface model has been  
656 tested . In this paper we focus on the assimilation of measured cosmic-ray neutron  
657 counts for improving soil moisture content characterization at the field scale. ~~The~~  
658 ~~assimilation of measured cosmic ray neutron counts in a land surface model has been~~  
659 ~~tested~~ (Han et al., 2014b; Rosolem et al., 2014a; Shuttleworth et al., 2013) = This paper  
660 focuses on the case that model input is biased. Land surface models still are affected  
661 by limited knowledge on water resources management and for regions in China (and  
662 elsewhere) typically no information on irrigation amounts is available as irrigation is  
663 mainly by the flooding system. We analyse whether measured neutron counts are able



664 to correct for such biases. This case is not only relevant for neglecting irrigation in  
665 China, but also for other water resources management issues (e.g., groundwater  
666 pumping) which are neglected in the simulations. Neglecting irrigation in land surface  
667 models results in a large bias in the simulated soil moisture content because of a lack  
668 of water input. The bias in soil moisture content also results in a too small latent heat  
669 flux and too high sensible heat flux. We hypothesize that data assimilation also can  
670 play an important role for removing such biases in data deficient areas. One possible  
671 strategy in data assimilation studies for handling this type of bias, which is not  
672 followed in this paper, is to calibrate the simulation model (e.g., land surface model)  
673 prior to data assimilation to remove biases (Kumar et al., 2012) and use the corrected  
674 simulation model in the context of sequential data assimilation. A different strategy ~~is~~  
675 was followed in this paper and no a priori bias correction ~~is~~was carried out because  
676 this type of problem (neglecting water resources management) does not allow for such  
677 an a priori bias correction~~does not allow for such an a priori bias correction. The bias~~  
678 can be contributed to the model structure, model parameter, atmospheric forcing or  
679 observation data, and the bias-aware assimilation requires the assumption that the bias  
680 comes from a particular source. If the source of bias is not attributed to the right  
681 source, model predictions cannot be improved~~Because~~The bias could~~can be~~  
682 ~~contributed to the model structure, model parameter, atmospheric forcing or~~  
683 ~~observation data, and the bias-aware assimilation requires the assumption that the bias~~  
684 ~~comes from a particular source~~ (Dee, 2005). Therefore bias-blind assimilation in  
685 which the bias estimation was not handled explicitly was used for safety. Instead, it

686 was investigated whether neutron counts measured by cosmic-ray probe were able to  
687 correct for the bias. ~~So Therefore the bias blind assimilation was used for safety.~~  
688 ~~Instead, it is investigated whether neutron counts measured by cosmic ray probe are~~  
689 ~~able to correct for the bias.~~ Aim is to improve the soil moisture profile estimation in a  
690 crop land with seed corn as main crop type.

691 In CLM, ~~the land~~ surface fluxes are calculated based on the Monin-Obukhov  
692 similarity theory. The sensible heat flux is formulated as a function of temperature and  
693 ~~leaf area index~~ LAI, and the latent heat flux is formulated as a function of the  
694 temperature and leaf stomatal resistances. The leaf stomatal resistance is calculated  
695 from the Ball-Berry conductance model (Collatz et al., 1991). The updates of soil  
696 temperature and vegetation temperature are derived based on the solar radiation  
697 absorbed by top soil (or vegetation), longwave radiation absorbed by soil (or  
698 vegetation), sensible heat flux from soil (or vegetation) and latent heat flux from soil  
699 (or vegetation). ~~And the m~~ Measured land surface temperature is composed of the  
700 ground temperature and vegetation temperature. Therefore a difference between  
701 measured and calculated land surface temperature can be adjusted by changing land  
702 surface fluxes. As land surface fluxes are sensitive to soil moisture content, land  
703 surface temperature is sensitive to soil moisture content. ~~Therefore T~~ the surface fluxes  
704 are therefore sensitive to the surface and soil land surface temperature.

705 ~~Beside of the cosmic ray neutron counts observation,~~ ~~Therefore, T~~ the land  
706 surface temperature (LST) products measured by the Moderate Resolution Imaging  
707 Spectroradiometer (MODIS) Terra (MOD11A1) and Aqua (MYD11A1) are also

708 assimilated jointly to improve the soil temperature profile estimation because the  
709 evapotranspiration is sensitive to the soil temperature. Two Terra LST products can be  
710 obtained per day at 10:30 am/pm and two Aqua LST products can be obtained per day  
711 at 1:30 am/pm. [Soil moisture, land surface temperature and LAI influence the](#)  
712 [estimation of latent and sensible heat fluxes](#) (Ghilain et al., 2012; Jarlan et al., 2008;  
713 Schwinger et al., 2010; van den Hurk, 2003; Yang et al., 1999) ~~(e.g., Ghilain et al.,~~  
714 ~~2012; Jarlan et al., 2008; Schwinger et al., 2010; van den Hurk et al., 2003; Yang et~~  
715 ~~al., 1999)~~, and therefore this study focuses in addition on the calibration of LAI with  
716 [help of the assimilation of land surface temperature](#). However, there are large  
717 [discrepancies between the remotely retrieved LAI and measured values, and the](#)  
718 [MODIS LAI product underestimates in situ measured LAI by 44% on average](#)  
719 [\(http://landval.gsfc.nasa.gov/\)](#), and therefore the LAI is also calibrated by data  
720 ~~assimilation. Soil moisture, land surface temperature and leaf area index LAI~~  
721 ~~contribute to the estimation of latent and sensible heat fluxes~~ (Ghilain et al., 2012;  
722 Jarlan et al., 2008; Schwinger et al., 2010; van den Hurk, 2003; Yang et al., 1999), ~~and~~  
723 ~~therefore this study focuses in addition on the calibration of leaf area index LAI using~~  
724 ~~the land surface temperature assimilation~~. However, there are large discrepancies  
725 ~~between the remotely retrieved LAI and measured values, and the MODIS LAI~~  
726 ~~product underestimates 44% of field measurement on average~~  
727 ~~(http://landval.gsfc.nasa.gov/)~~, and therefore the leaf area index LAI is also calibrated  
728 ~~by data assimilation~~. In summary, the novel aspects of this work are: 1) investigating  
729 whether data assimilation is able to correct for missing water resources management

730 data without a priori bias correction; 2) joint assimilation of cosmic-ray neutron  
731 counts, LST and updating of LAI; 3) application of this framework to real-world data  
732 in an irrigated area with the availability of detailed verification data; 733

733

## 734 **2. Materials and Methods**

### 735 **2.1 Study Area and Measurement**

736 The Heihe River Basin is the second largest inland river basin of China, and it is  
737 located between 97.1° E-102.0° E and 37.7° N-42.7° N and covers an area of  
738 approximately 143,000 km<sup>2</sup> (Li et al., 2013). In 2012, a multi-scale observation  
739 experiment of evapotranspiration with a well-equipped superstation (Daman  
740 superstation) to measure the atmospheric forcings and soil moisture at 2 cm, 4 cm, 10  
741 cm, 20 cm, 40 cm, 80 cm, 120 cm and 160 cm depth (Xu et al., 2013), was carried out  
742 from June to September in the framework of the Heihe Watershed Allied Telemetry  
743 Experimental Research (HiWATER) (Li et al., 2013). SoilNet wireless network nodes  
744 (Bogena et al., 2010) were deployed to measure soil moisture content and soil  
745 temperature at four layers (4 cm, 10 cm, 20 cm and 40 cm). One cosmic-ray soil  
746 moisture probe (CRS-1000B) was installed (Han et al., 2014c) with 23 SoilNet nodes  
747 (Jin et al., 2014; Jin et al., 2013) in the footprint (Fig. 1). The main crop type within  
748 the footprint of the cosmic-ray probe is seed corn. The irrigation is applied through  
749 channels using the flooding irrigation method. Exact amounts of applied irrigation are  
750 therefore not available.

751 The measured cosmic-ray neutron count data were processed to remove the

752 outliers according to the sensor voltage ( $\leq 11.8$  Volt) and relative humidity ( $\geq 80\%$ ).  
753 The surface fluxes were measured using the eddy covariance technique, and data were  
754 processed using EdiRe (<http://www.geos.ed.ac.uk/abs/research/micromet/EdiRe>)  
755 software, in which the anemometer coordinate rotation, signal lag removal, frequency  
756 response correction, density corrections and signal de-spiking were done for the raw  
757 data. The energy balance closure was not considered in this study. The ~~leaf-area~~  
758 ~~index~~LAI was measured by the LAI-2000 scanner during the field experiment, there  
759 are 17 samples collected in 14 days of 3 months.

760 [\[Insert Figure 1 here\]](#)

761

## 762 **2.2 Land Surface Model and Data**

763 The ~~Community Land Model~~ (CLM) was used to simulate the spatio-temporal  
764 distribution of soil moisture, soil temperature, land surface temperature, vegetation  
765 temperature, sensible heat flux, latent heat flux and soil heat flux of the study area.  
766 The coupled water and energy balance are modeled in CLM, and the land surface  
767 heterogeneity is represented by patched plant functional types and soil texture (Oleson  
768 et al., 2013).

769 The soil properties used in CLM were from the soil database of China with 1 km  
770 spatial resolution (Shangguan et al., 2013). The MODIS 500 m resolution plant  
771 functional type product (MCD12Q1) (Sun et al., 2008) which was resampled by  
772 nearest neighbor interpolation to 1 km resolution and MODIS ~~leaf-area-index~~LAI  
773 product (MCD15A3) with 1 km spatial resolution (Han et al., 2012) were used as

774 input. Due to a lack of measurement data, two atmospheric forcing data sets were  
775 used: the Global Land Data Assimilation System reanalysis data (Rodell et al., 2004)  
776 was interpolated using the National Centers for Environmental Prediction (NCEP)  
777 bilinear interpolation library iplib in spatial and temporal dimensions and used in the  
778 CLM for the spin-up period  
779 ([http://www.nco.ncep.noaa.gov/pmb/docs/libs/ipilib/ncep\\_ipilib.sht-ml](http://www.nco.ncep.noaa.gov/pmb/docs/libs/ipilib/ncep_ipilib.sht-ml)). For the three  
780 months data assimilation period, hourly forcing data (incident longwave radiation,  
781 incident solar radiation, precipitation, air pressure, specific humidity, air temperature  
782 and wind speed) from the Daman superstation of HiWATER were available and used.

783

### 784 **2.3 Cosmic-Ray Forward Model**

785 In this study, the new developed COsmic-ray Soil Moisture Interaction Code  
786 (COSMIC) model (Shuttleworth et al., 2013) was used as the cosmic-ray forward  
787 model to simulate the cosmic-ray neutron count rate using the soil moisture profile as  
788 input. The effective measurement depth of the cosmic-ray soil moisture probe ranges  
789 from 12 cm (wet soils) to 76 cm (dry soils) (Zreda et al., 2008), within which 86% of  
790 the above-ground measured neutrons originate. COSMIC also calculates the effective  
791 sensor depth based on the cosmic-ray neutron intensity and the soil moisture profile  
792 values (Franz et al., 2012; Shuttleworth et al., 2013).

793 COSMIC makes several assumptions to calculate the number of fast neutrons  
794 reaching the cosmic-ray soil moisture probe ( $N_{COSMOS}$ ) at a near-surface measurement  
795 location, and the soil layer with a depth of 3 meters for the complete soil profile, was

796 discretized into 300 layers for the integration of Eq. 2 in COSMIC. The number of  
 797 fast neutrons reaching the cosmic-ray probe  $N_{COSMOS}$  is formulated as (Shuttleworth  
 798 et al., 2013):

$$799 \quad N_{COSMOS} = N \int_0^{\infty} \left\{ A(z) [\alpha \rho_s(z) + \rho_w(z)] \exp \left( - \left[ \frac{m_s(z)}{L_1} + \frac{m_w(z)}{L_2} \right] \right) \right\} dz \quad (1)$$

$$800 \quad A(z) = \left( \frac{2}{\pi} \right)^{\pi/2} \int_0^{\pi/2} \exp \left( \frac{-1}{\cos(\theta)} \left[ \frac{m_s(z)}{L_3} + \frac{m_w(z)}{L_4} \right] \right) d\theta \quad (2)$$

$$801 \quad \alpha = 0.405 - 0.102 \times \rho_s \quad (3)$$

$$802 \quad L_3 = -31.76 + 99.38 \times \rho_s \quad (4)$$

803 where  $N$  is the high energy neutron intensity (counts/hour),  $z$  denotes the soil  
 804 layer depth (m),  $\rho_s$  ~~denotes~~ the dry soil bulk density (g/cm<sup>3</sup>),  $\rho_w$  ~~denotes~~ the total  
 805 water density, including the lattice water (g/cm<sup>3</sup>) and  $\alpha$  denotes the ratio of fast  
 806 neutron creation factor.  $L_1$  is the high energy soil attenuation length with value of  
 807 162.0 g/cm<sup>2</sup>, ~~and~~  $L_2$  ~~denotes~~ the high energy water attenuation length of 129.1  
 808 g/cm<sup>2</sup>. In equation (2)  $\theta$  is the angle between the vertical below the detector and the  
 809 line between the detector and each point in the plane,  $m_s(z)$  and  $m_w(z)$  are the  
 810 integrated mass per unit area of dry soil and water (g/cm<sup>2</sup>), respectively.  $L_3$  denotes  
 811 the fast neutron soil attenuation length (g/cm<sup>2</sup>) and  $L_4$  stands for the fast neutron  
 812 water attenuation length with value of 3.16 g/cm<sup>2</sup>.

813 The cosmic-ray neutron intensity reaching the land surface is influenced by air  
 814 pressure, atmospheric water vapor content and incoming neutron flux. In order to  
 815 isolate the contribution of soil moisture content to the measured neutron density, it is  
 816 important to take these effects into account and the calibrated neutron count [intensity](#)

817 can be derived as follows:

$$818 \quad N_{Corr} = N_{Obs} \times f_p \times f_{wv} \times f_i \quad (5)$$

819 where  $N_{Corr}$  represents corrected neutron counts and  $N_{Obs}$  the measured  
820 neutron counts.  $f_p$  is the correction factor for air pressure,  $f_{wv}$  the correction  
821 factor for atmospheric water vapor and  $f_i$  the correction factor for incoming neutron  
822 flux.

823 The correction factor for air pressure  $f_p$  can be calculated as~~The correction~~  
824 ~~factor for air pressure  $f_p$  can be calculated as~~ (Zreda et al., 2012):

$$825 \quad f_p = \exp\left(\frac{P - P_0}{L}\right) \quad (6)$$

826 where  $P$  (mbar) is the local air pressure,  $P_0$  (mbar) the average air pressure  
827 during the measurement period and  $L$  (g/cm<sup>2</sup>) is the mass attenuation length for  
828 high-energy neutrons; the default value of 128 g/cm<sup>2</sup> was used ~~for~~in this study (Zreda  
829 et al., 2012).

830 The correction factor  $f_{wv}$  for atmospheric water vapor is calculated as (Rosolem  
831 et al., 2013):

$$832 \quad f_{wv} = 1 + 0.0054 \times (\rho_{v0} - \rho_{v0}^{ref}) \quad (7)$$

833 where  $\rho_{v0}$  (kg/m<sup>3</sup>) is the absolute humidity at the measurement time and  $\rho_{v0}^{ref}$   
834 (kg/m<sup>3</sup>) is the average absolute humidity during the measurement period.

835 Fluctuations in the incoming neutron flux should be removed because the  
836 cosmic-ray probe is designed to measure the neutron flux based on the incoming  
837 background neutron flux. The correcting factor  $f_i$  for the incoming neutron flux is  
838 calculated as:



839 
$$f_i = \frac{N_m}{N_{avg}} \quad (8)$$

840 where  $N_m$  is the measured incoming neutron flux and  $N_{avg}$  is the average  
841 incoming neutron flux during the measurement period. The measured data at the  
842 Jungfraujoch station in Switzerland at 3560 m (<http://cosray.unibe.ch/>) was used to  
843 calculate  $N_m$  and  $N_{avg}$ . The temporal (secular or diurnal) variations caused by the  
844 sunspot cycle could be removed after this correction (Zreda et al., 2012).

845 In this study, the soil moisture for the CRS footprint scale was calculated from the  
846 arithmetic mean of the 23 SoilNet soil moisture observations.~~In this study, the soil~~  
847 ~~moisture at for the CRS footprint scale was calculated from the arithmetic mean of the~~  
848 ~~23 SoilNet soil moisture observations.~~ The calibration of the high energy neutron  
849 intensity parameter  $N$  in equation (1) was done using the measured cosmic-ray  
850 neutron counts rate and averaged soil moisture content at the CRS footprint scale.  
851 Because lattice water was unknown for this site, a value of 3% was assumed in this  
852 study (Franz et al., 2012). Hourly soil moisture measurements for a period of 2.5  
853 months were used for COSMIC calibration. Inside the cosmic-ray probe footprint, the  
854 amount of applied irrigation was spatially variable due to the different management  
855 practice of each farmer. The gradient search algorithm L-BFGS-B (Zhu et al., 1997)  
856 was used to minimize the root mean square error of the differences between simulated  
857 cosmic-ray neutron counts (using measured soil moisture by SoilNet as input to  
858 COSMIC) and the measured neutron counts  $N_{Corr}$ . The optimized parameter value of  
859  $N$  was 615.96 counts/hour in this case.

860 The simulated soil moisture content for 10 CLM soil layers (3.8 m depth) was

861 used as input to COSMIC in order to simulate the corresponding neutron count  
862 intensity and compare it with the measured neutron count intensity. It should be  
863 mentioned that it is unlikely that anything beyond 1 m deep will substantially impact  
864 the results because the effective measurement depth of the cosmic-ray probe is  
865 between 12 and 76 cm. The COSMIC model assumes a more detailed soil profile.  
866 ~~COSMIC interpolates the soil moisture information from the ten CLM~~~~COSMIC,~~  
867 ~~interpolates the soil moisture information from the ten-CLM~~ soil layers to information  
868 for 300 soil layers of depth 1cm. The contribution of each soil layer to the measured  
869 neutron flux will change temporally depending on the soil moisture condition.  
870 Therefore the effective measurement depth of the cosmic ray probe will also change  
871 temporally. COSMIC calculates the vertically weighted soil moisture content based  
872 on the vertical distribution of soil moisture content.~~For the data assimilation, the~~  
873 ~~simulated soil moisture content for 10 soil layers (3.8 m depth) in CLM was used as~~  
874 ~~the input to COSMIC in order to simulate the corresponding cosmic ray neutron~~  
875 ~~counts and compare it with the measured neutron counts. It should be mentioned that~~  
876 ~~it is unlikely that anything beyond 1 m deep will substantially impact the results~~  
877 ~~because the effective measurement depth of cosmic ray probe is between 12 and 76~~  
878 ~~cm. The COSMIC model assumes a more detailed soil profile. In COSMIC, the soil~~  
879 ~~moisture information from the 10 layers from CLM was interpolated to information~~  
880 ~~for 300 layers based on the soil layer depth for stable numerical solution. The~~  
881 ~~contribution of each soil layer to the measured neutron flux will change temporally~~  
882 ~~depending on the soil moisture condition. So the effective measurement depth of the~~

883 ~~cosmic ray probe will also change temporally. COSMIC calculates as output also the~~  
884 ~~neutron count rate and the vertically weighted soil moisture content, which is~~  
885 ~~calculated with help of the effective sensor depth obtained from COSMIC based on~~  
886 ~~the vertical distribution of soil moisture contents at different depth.~~

887

## 888 **2.4 Two Source Formulation - TSF**

889 The land surface temperature products of MODIS are composed of a ground  
890 temperature and vegetation temperature component, which are however unknown.  
891 CLM models the ground temperature and vegetation temperature separately, but does  
892 not model the composed land surface temperature as seen by MODIS. The  
893 corresponding land surface temperature of CLM should therefore be modelled for  
894 data assimilation purposes. The two source formulation (Kustas and Anderson, 2009)  
895 was used in this study to calculate the land surface temperature from the MODIS view  
896 angle using ground temperature and vegetation temperature simulated by CLM:

$$897 \quad T_s = [F_c(\Phi)T_c^4 + (1 - F_c(\Phi)T_g^4)]^{1/4} \quad (9)$$

898 where  $T_s$  (K) is the composed surface temperature as seen by the MODIS sensor,  
899  $F_c(\Phi)$  is the fraction vegetation cover observed from the sensor view angle  $\Phi$   
900 (radians),  $T_c$  (K) is the vegetation temperature and  $T_g$  (K) is the ground temperature.  
901 (Kustas and Anderson, 2009):

$$902 \quad F_c(\Phi) = 1 - \exp\left(\frac{-0.5\Omega(\Phi)LAI}{\cos\Phi}\right) \quad (10)$$

903 where  $LAI$  is the leaf area index,  $\Omega(\Phi)$  is a clumping index to represent the  
904 nonrandom leaf area distributions of farmland or other heterogeneous land surfaces

905 (Anderson et al., 2005), and is defined as:

$$906 \quad \Omega(\Phi) = \frac{0.49\Omega_{\max}}{0.49 + (\Omega_{\max} - 0.49)\exp(k\theta^{3.34})} \quad (11)$$

$$907 \quad \Omega_{\max} = 0.49 + 0.51(\sin \Phi)^{0.05} \quad (12)$$

$$908 \quad k = -\{0.3 + [1.7 * 0.49 * (\sin \Phi)^{0.1}]^{14}\} \quad (13)$$

909

## 910 **2.5 Assimilation Approach**

911 The Local Ensemble Transform Kalman Filter (LETKF) was used as the  
912 assimilation algorithm, which is one of the square root variants of the ensemble  
913 Kalman filter (Evensen, 2003; Hunt et al., 2007; Miyoshi and Yamane, 2007). The  
914 model uncertainties are represented using the ensemble simulation of model states and  
915 LETKF derives the background error covariance using the model state ensemble  
916 members. LETKF uses the non-perturbed observations to update all the ensemble  
917 members of model states at each assimilation step.

918 In this study,  $x_1^b, \dots, x_N^b$  denote the model state ensemble members;  $\bar{x}^b$  is the  
919 ensemble mean of  $x_1^b, \dots, x_N^b$ ;  $N$  is the ensemble size;  $y_1^b, \dots, y_N^b$  denote the mapped  
920 model state ensemble members;  $\bar{y}^b$  is the ensemble mean of  $y_1^b, \dots, y_N^b$ ;  $H$  is the  
921 observation operator (COSMIC for soil moisture or the two source function for land  
922 surface temperature). The analysis step of LETKF can be summarized as follows:

923 Prepare the model state vector  $X^b$ :

$$924 \quad X^b = [x_1^b - \bar{x}^b, \dots, x_N^b - \bar{x}^b] \quad (14)$$

925 where  $\bar{x}^b$  is composed of one vertically weighted soil moisture content and soil  
926 moisture content for 10 CLM-layers, resulting in a state dimension equal to 11 if only

927 ~~the neutron count observation was assimilated~~~~the neutron counts observations were~~  
928 ~~assimilated~~; and  $\bar{x}^b$  is composed of surface temperature, ground temperature,  
929 vegetation temperature and soil temperature for 15 CLM-layers if only the land  
930 surface temperature observations were assimilated without soil moisture update,  
931 giving a state dimension of 18. The water and energy balance are coupled, and in  
932 CLM the energy balance is firstly solved, then the derived surface fluxes are used ~~in~~  
933 ~~for~~ updating ~~the~~ soil moisture content. ~~So~~ ~~+~~ ~~the~~ cross correlation between the soil  
934 temperature and soil moisture ~~could~~ can be calculated using the ensemble prediction  
935 in LETKF, and this makes the updating of soil moisture by assimilating land surface  
936 temperature possible. We also used the land surface temperature to update the soil  
937 moisture profile, in this case the soil moisture vector was augmented to the LETKF  
938 state vector of land surface temperature assimilation, ~~and~~ resulting in a state  
939 dimension of 28. For the calibration of the LAI, the state vector was augmented with  
940 surface temperature, ground temperature, vegetation temperature, soil temperature for  
941 15 CLM-layers and LAI if only the land surface temperature observations were  
942 assimilated without soil moisture update. This resulted then in a state dimension of  
943 19.~~For the calibration of the LAI, the state vector was augmented as surface~~  
944 ~~temperature, ground temperature, vegetation temperature, soil temperature for 15~~  
945 ~~CLM layer and LAI if only the land surface temperature observations were~~  
946 ~~assimilated without soil moisture update, giving a state dimension of 19.~~

947 Construct the mapped model state vector  $Y^b$  after transformation of observation  
948 operator:

949  $y_i^b = H(x_i^b)$  (15)

950  $Y^b = [y_1^b - \bar{y}^b, \dots, y_N^b - \bar{y}^b]$  (16)

951 The following analysis is looped for each model grid cell to calculate the update  
 952 of model state ensemble members:

953 Calculate analysis error covariance matrix  $P^a$ :

954  $P^a = [(N - 1)I + Y^{bT}R^{-1}Y^b]$  (17)

955 The perturbations in ensemble space are calculated as:

956  $W^a = [(N - 1)P^a]^{1/2}$  (18)

957 Calculate the analysis mean  $\bar{w}^a$  in ensemble space and add to each column of  
 958  $W^a$  to get the analysis ensemble in ensemble space:

959  $\bar{w}^a = P^a Y^{bT} R^{-1} (y^o - \bar{y}^b)$  (19)

960 Calculate the new analysis:

961  $X^a = X^b [\bar{w}^a + W^a] + \bar{x}^b$  (20)

962 where  $R$  is the observation error covariance matrix,  $y^o$  is the observation vector  
 963 and  $X^a$  contains the updated model ensemble members.

964 The LETKF method can also be extended to do parameter estimation using a state  
 965 augmentation approach (Bateni and Entekhabi, 2012; Li and Ren, 2011; Moradkhani  
 966 et al., 2005; Nie et al., 2011). Alternative strategies for parameter estimation are a dual  
 967 approach (Moradkhani et al., 2005) with separate updating of states and parameters.  
 968 Vrugt et al. (2005) also proposed a dual approach with parameter updating in an outer  
 969 optimization loop using [a Markov Chain Monte Carlo methods](#), and state updating in  
 970 an inner loop. The a priori calibration of model parameters is also an option (Kumar et

971 al., 2012). With the augmentation approach, the state vector of LETKF can be  
972 augmented by the parameter vector including soil properties (sand fraction, clay  
973 fraction and organic matter density) and vegetation parameters (~~leaf area index~~LAI,  
974 etc.). In a preliminary sensitivity study it was found that for this site simulation results  
975 were more sensitive to the ~~leaf area index~~LAI than to soil properties. Soil texture is  
976 also quite well known for this site from measurements. Therefore in this study, only  
977 the ~~leaf area index~~LAI was in some of the simulation scenarios calibrated. In the  
978 different scenarios of land surface temperature assimilation, the LETKF state vector  
979 was also augmented to include ~~leaf area index~~LAI as calibration target. As a  
980 consequence, the augmented state vector contains surface temperature, ground  
981 temperature, and vegetation temperature, 15 layers of soil temperature and ~~leaf area~~  
982 ~~index~~LAI, making up a state dimension equal to 19 for the scenarios of land surface  
983 temperature assimilation without soil moisture update; for the scenarios of land  
984 surface temperature with soil moisture update, the state dimension is 29~~for the~~  
985 ~~scenarios of land surface temperature with soil moisture update, the state dimension~~  
986 ~~will be changed to 29.~~ The 10 layers of soil moisture and 15 layers of soil temperature  
987 are the standard CLM layout for both soil moisture and soil temperature. The  
988 hydrology calculations are done over the top 10 layers, and the bottom 5 layers are  
989 specified as bedrock. The lower 5 layers are hydrologically inactive layers.  
990 Temperature calculations are done over all layers (Oleson et al., 2013).

991

### 992 3. Experiment Setup

993 First~~ly~~ the 50 ensemble members of CLM with perturbed soil properties and  
994 atmospheric forcing data were driven from the 1<sup>st</sup> of Jan. 2012 to the 31<sup>st</sup> of May 2012  
995 to do the CLM spin-up; second~~ly~~ an additional assimilation period of cosmic-ray  
996 neutron counts was done from the 1<sup>st</sup> of Jun. 2012 to the 30<sup>th</sup> Aug. 2012 to reduce the  
997 spin-up error. Then the final CLM states on 30<sup>th</sup> Aug. 2012 were used as the initial  
998 states for the following data assimilation scenarios. Perturbed soil properties were  
999 generated by adding a spatially uniform perturbation sampled from a uniform  
1000 distribution between -10% and 10% to the values extracted from the Soil Database of  
1001 China for Land Surface Modeling (1 km spatial resolution). The LAI was perturbed  
1002 with multiplicative uniform distributed random noise in the range of [0.8~1.2]. The  
1003 perturbations added to the model forcings show correlations in space and time~~The leaf~~  
1004 ~~area index was perturbed with multiplicative uniform distributed random noise in the~~  
1005 ~~range of [0.8~1.2]. The model forcings were perturbed by adding a perturbation,~~  
1006 ~~showing correlations in space and time.~~ The spatial correlation was induced by a Fast  
1007 Fourier Transform and the temporal correlation by a first-order auto-regressive model  
1008 (Han et al., 2013; Kumar et al., 2009; Reichle et al., 2010). The statistics on the  
1009 perturbation of the forcing data are summarized in Table 1. The values of standard  
1010 deviations and temporal correlations in Table 1 were chosen based on previous  
1011 catchment scale and regional scale data assimilation studies~~data assimilation~~ (De  
1012 Lannoy et al., 2012; Kumar et al., 2012; Reichle et al., 2010).

1013 [Insert Table 1 here]

1014 The cosmic-ray neutron intensity was assimilated every 3 days at 12Z from the 1<sup>st</sup>



1015 of June 2012 onwards, because we found that the difference between daily  
1016 assimilation and 3 days assimilation was small (Entekhabi et al., 2010; Kerr et al.,  
1017 2010). The measured neutron count intensity showed large temporal fluctuations in  
1018 time and these fluctuations were not corresponding to the temporal variations of soil  
1019 moisture. Therefore the measured neutron count intensity was smoothed with the  
1020 Savitzky–Golay filter using a moving average window of size 31 hours and a  
1021 polynomial of order 4 (Savitzky and Golay, 1964). The originally measured neutron  
1022 counts and smoothed neutron counts are plotted in Fig. 2. The assimilation frequency  
1023 of MODIS LST products of MOD11A1 and MYD11A1 was up to 4 times (maximum)  
1024 per day depending on the data availability. There are 230 observation data (including  
1025 cosmic-ray probe neutron counts, MODIS LST, MOD11A1 and MYD11A1 LST) in  
1026 the whole assimilation window. The variance of the instantaneous measured neutron  
1027 intensity was equal to the measured neutron count intensity (Zreda et al., 2012) and  
1028 smaller for temporal averaging for daily or sub-daily applications. (Zreda et al., 2012)  
1029 The instantaneous neutron intensity was assimilated in this study. and tThe variance  
1030 of MODIS LST was assumed to be 1 K. (Wan and Li, 2008)(Wan and Li, 2008).The  
1031 variance of Cosmic ray was the measured neutron counts value (Zreda et al., 2012)  
1032 and the variance of MODIS LST was assumed to be 1 K.

1033 The 4 days MODIS ~~leaf area index~~LAI product was aggregated and used as the  
1034 CLM ~~leaf area index~~LAI parameter. Because the ~~leaf area index~~LAI from MODIS is  
1035 usually lower than the true value (compared with the field measured ~~leaf area~~  
1036 ~~index~~LAI in the HiWATER experiment) and because the surface flux and surface

1037 temperature are sensitive to the ~~leaf-area-index~~LAI, two additional scenarios were  
1038 investigated where ~~leaf-area-index~~LAI was calibrated to study the impact of ~~leaf-area~~  
1039 ~~index~~LAI estimation on surface flux estimation within the data assimilation  
1040 framework.

1041 The following assimilation scenarios were compared: (1) CLM: open loop  
1042 simulation without assimilation; (2) Only\_CRS: only the measured neutron counts  
1043 were assimilated; (3) Only\_LST: only the MODIS LST products were assimilated.  
1044 The quality control flags of LST products were used to select the data with good  
1045 quality for assimilation; (4) CRS\_LST: the measured neutron counts and MODIS LST  
1046 products were assimilated jointly. In the above scenarios, the neutron count data was  
1047 used to update the soil moisture and the LST data were used to update the ground  
1048 temperature, vegetation temperature and soil temperature. (5) LST\_Feedback: We also  
1049 evaluated the scenario of assimilating the LST measurements to update the soil  
1050 moisture profile. (6) CRS\_LST\_Par\_LAI: the ~~leaf-area-index~~LAI was included as  
1051 variable to be calibrated, otherwise the scenario was the same as CRS\_LST. (7)  
1052 LST\_Feedback\_Par\_LAI: the ~~leaf-area-index~~LAI was included as variable to be  
1053 calibrated, otherwise the scenario was the same as LST\_Feedback. (8)  
1054 CRS\_LST\_True\_LAI: the in situ measured ~~leaf-area-index~~LAI during the HiWATER  
1055 experiment was used in the model simulation.

1056 [\[Insert Figure 2 here\]](#)

1057

## 1058 **4. Results and Discussion**

1059 In order to evaluate the assimilation results for the different scenarios outlined in  
1060 section 3, the Root Mean Square Error (RMSE) was used:

$$1061 \quad \text{RMSE} = \sqrt{\frac{\sum_{n=i}^N (\text{Estimated} - \text{Measured})^2}{N}} \quad (21)$$

1062 where “*Estimated*” is the ensemble mean without assimilation or the ensemble  
1063 mean after assimilation, “*Measured*” is measured soil moisture content evaluated at  
1064 the SoilNet nodes (or latent heat flux, sensible heat flux or soil heat flux).  $N$  is the  
1065 number of time steps. For the soil moisture analysis in this study,  $N$  is equal to 2184.  
1066 The smaller the RMSE value is, the closer assimilation results are to measured values,  
1067 which is in general considered to be desirable.

1068 The temporal evolution of soil moisture content at 10, 20, 50 and 80 cm depth for  
1069 different ~~scenarios~~ scenarios is plotted in Fig. 3 and Fig. 4. The RMSE values for  
1070 different scenarios are summarized in Table 2. Assimilating the land surface  
1071 temperature could improve the soil moisture profile estimation in the scenario of  
1072 LST\_Feedback\_Par\_LAI; the soil moisture results are better than the open loop run at  
1073 all depths. With the assimilation of CRS neutron counts, the soil moisture RMSE  
1074 values (scenarios CRS\_LST\_Par\_LAI and CRS\_LST\_True\_LAI) decreased  
1075 significantly. The RMSE values for the scenarios Only\_CRS and CRS\_LST (not  
1076 shown) are similar to CRS\_LST\_Par\_LAI, which indicates that the main  
1077 improvement for the soil moisture profile characterization is achieved by neutron  
1078 count assimilation; and land surface temperature assimilation and ~~leaf area index~~LAI  
1079 estimation play a minor role. Without assimilation of cosmic-ray probe neutron counts,  
1080 the soil moisture simulation cannot be improved (scenario Only\_LST). However, the

1081 scenarios of LST Feedback and LST Feedback Par LAI improve the soil moisture  
1082 profile characterization, which shows that explicitly using LST to update soil moisture  
1083 content in the data assimilation routine gives better results than using LST only to  
1084 update soil moisture by the model equations.~~Without assimilation of cosmic-ray probe~~  
1085 ~~neutron counts, the soil moisture simulation cannot be improved in the scenario~~  
1086 ~~Only\_LST. However, the scenarios of LST\_Feedback and LST\_Feedback\_Par\_LAI~~  
1087 ~~improve the soil moisture profile characterization, which shows that explicitly using~~  
1088 ~~LST to update soil moisture content in the data assimilation routine gives better~~  
1089 ~~results than using LST only to update soil moisture over the model equations.~~ Results  
1090 of LST\_Feedback and LST\_Feedback\_Par\_LAI are similar; therefore only results for  
1091 LST\_Feedback\_Par\_LAI are shown in Fig. 3 and Fig. 4. This implies that the  
1092 improved soil moisture characterization due to LAI calibration is low. The results for  
1093 the cosmic-ray probe neutron count assimilation proved that the cosmic-ray probe  
1094 sensor can be used to improve the soil moisture profile estimation at the footprint  
1095 scale~~The results for the cosmic ray probe neutron count assimilation proved the~~  
1096 ~~cosmic-ray probe sensor can be used to improve the soil moisture profile estimation at~~  
1097 ~~the footprint scale.~~

1098 [Insert Figure 3 here]

1099 [Insert Figure 4 here]

1100 [Insert Table 2 here]

1101 Fig. 5 depicts the scatter plots of measured ET versus modelled ET for different  
1102 scenarios, and the accumulated ET for all scenarios are summarized in the lower-right

1103 corner of Fig. 5. The EC measured evapotranspiration (ET) is 384.7 mm for the  
1104 assimilation period, without energy balance closure correction. The true  
1105 evapotranspiration is therefore likely larger, but not much larger as the energy balance  
1106 gap was limited (3.7%). The CLM estimated ET, without data assimilation, using only  
1107 precipitation as input is 223.7 mm and is much smaller than the measured value as  
1108 applied irrigation is not considered in the model. This open loop simulated value  
1109 would imply water stress and a limitation of canopy transpiration and soil evaporation  
1110 due to low soil moisture content. Assimilation of land surface temperature only  
1111 (Only\_LST) hardly affected the estimated ET and was not able to correct for the  
1112 artificial water stress condition. However, if land surface temperature was used to  
1113 update soil moisture directly, taking into account correlations between the two states  
1114 in the data assimilation routine, the ET estimates improved to 336.8 mm and 354.8  
1115 mm for the scenarios of LST\_Feedback and LST\_Feedback\_Par\_LAI respectively.  
1116 The assimilation of land surface temperature of MODIS with soil moisture update  
1117 results in significant improvements of ET.

1118 The different neutron count assimilation scenarios also resulted in significantly  
1119 improved estimates of ET. Univariate assimilation of cosmic-ray neutron data  
1120 (Only\_CRS) resulted in 301.9 mm ET. This shows that the impact of neutron count  
1121 assimilation to correct evapotranspiration estimates is little smaller than the impact of  
1122 land surface temperature with soil moisture update. Joint assimilation of land surface  
1123 temperature data and cosmic-ray neutron data (CRS\_LST) gave a slightly larger ET of  
1124 310.6 mm than Only\_CRS. Scenarios of CRS\_LST\_Par\_LAI and

1125 CRS\_LST\_True\_LAI gave the best ET estimates (360.5 mm and 349.3 mm). This  
1126 shows that correcting the biased LAI-estimates from MODIS by in situ data or  
1127 calibration helped to improve model estimates.

1128 [\[Insert Figure 5 here\]](#)

1129 The RMSE values of latent heat flux, sensible heat flux and soil heat flux for all  
1130 scenarios are summarized in Fig. 6, ~~Fig. 7, Fig. 8 and Table 3~~. It is obvious that the  
1131 RMSE values are very large for both the latent heat flux (123.9 W/m<sup>2</sup>) (~~Fig. 6~~) and  
1132 sensible heat flux (80.5 W/m<sup>2</sup>) (~~Fig. 7~~) for the open loop run and all other scenarios  
1133 where the soil moisture was not updated. If the land surface temperature was  
1134 assimilated to update the soil moisture, the latent heat flux RMSE decreased to 60.5  
1135 W/m<sup>2</sup> (LST\_Feedback) and 62.5 W/m<sup>2</sup> (LST\_Feedback\_Par\_LAI). [The scenario](#)  
1136 [where soil moisture and LAI are jointly updated \(LST Feedback Par LAI\) gave](#)  
1137 [worse results than the scenario of LST Feedback.](#)~~The joint soil moisture and LAI~~  
1138 ~~update scenario of LST Feedback Par LAI was worse than the single soil moisture~~  
1139 ~~update scenario of LST Feedback in this case.~~ Again, the assimilation of neutron  
1140 counts also resulted in a strong RMSE reduction for the latent heat flux (76.5 W/m<sup>2</sup>  
1141 for Only\_CRS). If in addition land surface temperature was assimilated and ~~leaf area~~  
1142 ~~index~~[LAI](#) optimized, the RMSE value of latent heat flux further decreased to 56.1  
1143 W/m<sup>2</sup> (70.7 W/m<sup>2</sup> without LAI optimization). If the field measured LAI was used  
1144 instead in the assimilation (CRS\_LST\_True\_LAI), the RMSE was 61.0 W/m<sup>2</sup>. These  
1145 results are in correspondence with the ones discussed before for soil moisture  
1146 characterization. Evidently, the combined assimilation of cosmic-ray probe neutron

1147 counts and land surface temperature, and calibration of ~~leaf-area-index~~LAI (or use of  
1148 field measured ~~leaf-area-index~~LAI as model input) shows the strongest improvement  
1149 for the estimation of land surface fluxes. The soil heat flux did not show a clear  
1150 improvement related to assimilation and showed only some improvement in case LAI  
1151 was calibrated ~~(Fig. 8)~~. For the scenario of land surface temperature assimilation  
1152 without soil moisture update (Only\_LST), estimates of latent and sensible heat flux  
1153 are not improved. It means that under water stress condition, the improved  
1154 characterization of land surface temperature (and soil temperature) does not contribute  
1155 to a better estimation of land surface fluxes.

1156 ~~{Insert Table 3 here}~~

1157 [Insert Figure 6 here]

1158 ~~{Insert Figure 7 here}~~

1159 ~~{Insert Figure 8 here}~~

1160 The updated ~~leaf-area-index~~LAI for scenarios of LST\_Feedback\_Par\_LAI and  
1161 CRS\_LST\_Par\_LAI is shown in Fig. ~~97~~. The MODIS ~~leaf-area-index~~LAI product was  
1162 used as input for CLM and time series are plotted as blue line in Fig. ~~9-7~~  
1163 (Background). The ~~leaf-area-index~~LAI was also measured in the HiWATER  
1164 experiment, and the measured values are shown as green star (Observation).  
1165 Ens\_Mean represents the mean ~~leaf-area-index~~LAI of all ensemble members  
1166 (Ensembles). It is obvious that MODIS underestimates the ~~leaf-area-index~~LAI  
1167 compared with the observations. With the assimilation of land surface temperature,  
1168 the ~~leaf-area-index~~LAI could be updated and be closer to the observations, but there is

1169 still a significant discrepancy between the measured ~~leaf-area-index~~LAI and the  
1170 updated one. The ~~leaf-area-index~~LAI values for the scenario with ~~leaf-area-index~~LAI  
1171 calibration (CRS\_LST\_Par\_LAI) are close to the measured ~~leaf-area-index~~LAI values  
1172 (CRS\_LST\_True\_LAI), which is an encouraging result. The calibrated ~~leaf-area~~  
1173 ~~index~~LAI shows some unrealistic increases and decreases during the assimilation  
1174 period, which is inherent to the data assimilation approach. A smoothed representation  
1175 of the ~~leaf-area-index~~LAI might provide a more realistic picture.

1176 [\[Insert Figure 7 here\]](#)

1177 This study illustrates that for an irrigated farmland, the measured cosmic-ray  
1178 probe neutron counts can be used to improve the soil moisture profile estimation  
1179 significantly. Without irrigation data, CLM underestimated soil moisture content. The  
1180 cosmic-ray neutron count data assimilation can be used as an alternative way to  
1181 retrieve the soil moisture content profile in CLM. The improved soil moisture  
1182 simulation was helpful for the characterization of the land surface fluxes  
1183 characterization. The univariate assimilation of land surface temperature without soil  
1184 moisture update is not helpful for the estimation of land surface fluxes and even  
1185 worsened the sensible heat flux characterization (Fig. ~~76~~). However, in a multivariate  
1186 data assimilation framework where land surface temperature was assimilated together  
1187 with measured cosmic-ray probe neutron counts, the land surface temperature  
1188 assimilation contributed significantly to an improved ET estimation. The simulated  
1189 canopy transpiration in CLM was in general too low, even when the water stress  
1190 condition was corrected by assimilating neutron counts, which was related to small



1191 values of the ~~leaf area index~~LAI. The additional estimation of ~~leaf area index~~LAI  
1192 through the land surface temperature assimilation resulted in an increase of the ~~leaf~~  
1193 ~~area index~~LAI yielding an increase of estimated ET.

1194 In general, land surface models need to be calibrated before use in land data  
1195 assimilation, especially if there is an apparent large bias in the model simulation (Dee,  
1196 2005). The simulation of soil moisture and surface fluxes was biased in our study,  
1197 mainly due to the lack of irrigation water as input. This bias cannot be corrected a  
1198 priori without exact irrigation data, which are not available in the field. The data  
1199 assimilation was proven to be an efficient way to remove the model bias in this case.  
1200 We also calculated the equivalent water thickness to analyze the equivalent irrigated  
1201 water after each step of soil moisture update. For the scenarios of CRS\_LST\_Par\_LAI  
1202 and CRS\_LST\_True\_LAI, the equivalent irrigation in three months was 693.6 mm  
1203 and 607.6 mm, respectively. Because the irrigation method is flood irrigation, it is not  
1204 easy to evaluate the true irrigation applied in the field. From the results we see  
1205 however that the applied irrigation (in the model) is much larger than actual ET  
1206 (~600-700mm vs ~400mm)~~(~700mm vs ~400mm)~~. This could indicate that the  
1207 amount of applied irrigation in the model is too large, but irrigation by flooding is also  
1208 inefficient and results in excess runoff and infiltration to the groundwater, because it  
1209 cannot be controlled so well as sprinkler irrigation or drip irrigation. Therefore, the  
1210 calculated amount of irrigation could be realistic, but might also be too large if soil  
1211 properties are erroneous in the model.

1212 The soil moisture content measured by the cosmic-ray probe represents the depth

1213 between 12 cm (very humid) and 76 cm (extremely dry case) depending on the  
1214 amount of soil water (soil moisture content and lattice water). Therefore the effective  
1215 sensor depth of the cosmic-ray probe will change over time. In order to model the  
1216 variable sensor depth and the relationship between the soil moisture content and  
1217 neutron counts, the new developed COSMIC model was used as the observation  
1218 operator in this study. Additionally the influences of air pressure, atmospheric vapor  
1219 pressure and incoming neutron counts were removed from the original measured  
1220 neutron counts. Because there is still some water in the crop which also affects the  
1221 cosmic-ray probe sensor, the COSMIC observation operator could be improved to  
1222 include vegetation effects. Several default parameters proposed by (Shuttleworth et al.,  
1223 2013) were used in the COSMIC model, these parameters probably need further  
1224 calibration following the development of the COSMIC model.

1225 The spatial distribution of soil moisture for the study area was very  
1226 heterogeneous due to the small farmland patches and different irrigation periods for  
1227 the different farmlands. Therefore the soil moisture content inferred by SoilNet may  
1228 not represent the true soil moisture content of the cosmic-ray probe footprint, which is  
1229 a further limitation of this study. Although the Cosmic-ray Soil Moisture Observing  
1230 System (COSMOS) has been designed as a continental scale network by installing  
1231 500 COSMOS probes across the USA (Zreda et al., 2012), there are still some  
1232 disadvantages of COSMOS compared with remote sensing. COSMOS is also  
1233 expensive for extensive deployment to measure the continental/regional scale soil  
1234 moisture.~~there are still some disadvantages of COSMOS compared with remote~~

1235 ~~sensing. The land surface is heterogeneous and COSMOS only samples part of this~~  
1236 ~~heterogeneity. COSMOS is also expensive for extensive deployment. Although the~~  
1237 ~~Cosmic ray Soil Moisture Observing System (COSMOS) has been designed as a~~  
1238 ~~continental scale network by installing 500 COSMOS probes across the USA (Zreda~~  
1239 ~~et al., 2012). But there are still some disadvantages of COSMOS compared with the~~  
1240 ~~remote sensing. Because the land surface is heterogeneous and COSMOS only catch~~  
1241 ~~the heterogeneity of local footprint scale, and COSMOS is expensive for extensive~~  
1242 ~~deployment.~~

## 1243 5. Summary and Conclusions

1244 In this paper, we studied the univariate assimilation of MODIS land surface  
1245 temperature products, the univariate assimilation of measured neutron counts by the  
1246 cosmic-ray probe, the bivariate assimilation of land surface temperature and neutron  
1247 count data, and the additional calibration of ~~leaf area index~~LAI for an irrigated  
1248 farmland at the Heihe catchment in China, where data on the amount of applied  
1249 irrigation were lacking. The most important objective of this study was to test whether  
1250 data assimilation is able to correct for the absence of information on water resources  
1251 management as model input, a situation commonly encountered in large scale land  
1252 surface modelling. For the specific case of lacking irrigation data, no ~~a-priori~~ bias  
1253 correction is possible. ~~The bias blind assimilation without explicit bias estimation was~~  
1254 ~~used. We focused on the model bias introduced by the forcing data and the LAI, and~~  
1255 ~~neglected the other sources of bias.~~ In case ~~leaf area index~~LAI was calibrated, this  
1256 was done at each data assimilation step of land surface temperature. The data

1257 assimilation experiments were carried out with the ~~Community Land Model (CLM)~~  
1258 and the data assimilation algorithm used was the ~~Local Ensemble Transform Kalman~~  
1259 ~~Filter (LETKF)~~. A likely further model bias, besides missing information on irrigation,  
1260 is the underestimation of LAI by MODIS, which was used to force the model.

1261 The results show that the direct assimilation of measured cosmic-ray neutron  
1262 counts improves the estimation of soil moisture significantly, whereas univariate  
1263 assimilation of land surface temperature without soil moisture update does not  
1264 improve soil moisture estimation. However, if the land surface temperature was  
1265 assimilated to update the soil moisture profile directly with help of the state  
1266 augmentation method, the evapotranspiration and soil moisture could be improved  
1267 significantly. This result suggests that the land surface temperature remote sensing  
1268 products are needed to correct the characterization of the soil moisture profile and the  
1269 evapotranspiration. The improved soil moisture estimation after the assimilation of  
1270 neutron counts resulted in a better ET estimation during the irrigation season,  
1271 correcting the too low ET of the open loop simulation. The joint assimilation of  
1272 neutron counts and MODIS land surface temperature improved the ET estimation  
1273 further compared to neutron count assimilation only. The best ET estimation was  
1274 obtained for the joint assimilation of cosmic-ray neutron counts, MODIS land surface  
1275 temperature including calibration of the ~~leaf area index~~LAI (or if field measured ~~leaf~~  
1276 ~~area index~~LAI was used as input). This shows that bias due to neglected information  
1277 on water resources management can be corrected by data assimilation if a  
1278 combination of soil moisture and land surface temperature data is available.

1279 We can conclude that data assimilation of neutron counts and land surface  
1280 temperature is useful for ET and soil moisture estimation of an irrigated farmland,  
1281 even if irrigation data are not available and excluded from model input. The land  
1282 surface temperature measurements are an alternative data source to improve the soil  
1283 moisture and land surface fluxes estimation under water stress conditions. This shows  
1284 the potential of data assimilation to correct also a systematic model bias. ~~Leaf-area~~  
1285 ~~index~~LAI optimization further improves simulation results, which is also likely  
1286 related to a systematic underestimation of LAI by the MODIS remote sensing product.  
1287 The results of using the calibrated ~~leaf-area-index~~LAI are comparable to the results of  
1288 using field measured ~~leaf-area-index~~LAI as model input.

1289

## 1290 **Acknowledgements**

1291 This work is supported by the NSFC (National Science Foundation of China)  
1292 project (grant number: 41271357, 91125001), the Knowledge Innovation Program of  
1293 the Chinese Academy of Sciences (grant number: KZCX2-EW-312) and the  
1294 Transregional Collaborative Research Centre 32, financed by the German Science  
1295 foundation. JungfrauJoch neutron monitor data were kindly provided by the  
1296 Cosmic-ray Group, Physikalisches Institut, University of Bern, Switzerland. We  
1297 acknowledge computing resources and time on the Supercomputing Center of Cold  
1298 and Arid Region Environment and Engineering Research Institute of Chinese  
1299 Academy of Sciences.

1300

1301 **List of Tables**

1302 Table 1 Summary of perturbation parameters for atmospheric forcing data.

1303

1304 Table 2 Root Mean Square Error (RMSE) of soil moisture profile of open loop run  
1305 (CLM), feedback assimilation of land surface temperature including LAI calibration  
1306 (LST\_Feedback\_Par\_LAI), bivariate assimilation of neutron counts and land surface  
1307 temperature including LAI calibration (CRS\_LST\_Par\_LAI) and bivariate  
1308 assimilation of neutron counts and land surface temperature (CRS\_LST\_True\_LAI).

1309

1310 ~~Table 3 Root Mean Square Error (RMSE) of latent heat flux and sensible heat flux for~~  
1311 ~~different simulation scenarios.~~

Table 1 Summary of perturbation parameters for atmospheric forcing data

<b>Variables</b>	<b>Noise</b>	<b>Standard deviation</b>	<b>Time Correlation scale</b>	<b>Spatial Correlation Scale</b>	<b>Cross correlation</b>
Precipitation	Multiplicative	0.5	24 h	5 km	[ 1.0,-0.8, 0.5, 0.0,
Shortwave radiation	Multiplicative	0.3	24 h	5 km	-0.8, 1.0,-0.5, 0.4,
Longwave radiation	Additive	20 W/m <sup>2</sup>	24 h	5 km	0.5, -0.5, 1.0, 0.4,
Air temperature	Additive	1 K	24 h	5 km	0.0, 0.4, 0.4, 1.0]

1313

1314

1315 Table 2 Root Mean Square Error (RMSE) of soil moisture profile of open loop run  
 1316 (CLM), feedback assimilation of land surface temperature including LAI calibration  
 1317 (LST\_Feedback\_Par\_LAI), bivariate assimilation of neutron counts and land surface  
 1318 temperature including LAI calibration (CRS\_LST\_Par\_LAI) and bivariate  
 1319 assimilation of neutron counts and land surface temperature using ground-based  
 1320 measured LAI as input (CRS\_LST\_True\_LAI).

Soil Layer Depth	RMSE (m <sup>3</sup> /m <sup>3</sup> )			
	Open Loop (CLM)	LST_Feedback _Par_LAI	CRS_LST _Par_LAI	CRS_LST _True_LAI
10 cm	0.202	0.137	0.085	0.086
20 cm	0.167	0.106	0.047	0.048
50 cm	0.193	0.112	0.112	0.119
80 cm	0.188	0.124	0.136	0.146

1321

1322



1323

Table 3 Root Mean Square Error (RMSE) of latent heat flux and sensible heat flux for

1324

different simulation scenarios.

<b>Scenarios</b>	<b>RMSE (W/m<sup>2</sup>)</b>	
	<b>Latent Heat</b>	<b>Sensible Heat</b>
Open-Loop (CLM)	123.9	80.5
LST_Feedback	60.5	34.8
LST_Feedback_Par_LAI	62.5	37.2
Only_CRS	76.5	43.3
CRS_LST	70.7	40.5
CRS_LST_Par_LAI	56.1	31.9
CRS_LST_True_LAI	61.0	34.5

1325

---

1326 **List of Figures**

1327 Figure 1. Map of the cosmic-ray probe and SoilNet Nodes in the footprint of the CRS  
1328 probe positioned at the Heihe river catchment

1329

1330 Figure 2. Measured and temporally smoothed CRS neutron counts

1331

1332 Figure 3. Soil moisture at 10 cm (upper) and 20 cm (lower) depth as obtained from an  
1333 open loop run (CLM), local sensors (Obs), and different simulation scenarios. For a  
1334 description of the scenarios see section 3 of the paper. The CRS neutron counts were  
1335 assimilated from the 1st of June

1336

1337 Figure 4. ~~Same as figure 3 but for 50 cm and 80 cm. Soil moisture at 50 (upper) cm-~~  
1338 ~~and 80 cm (lower) depth measured and modeled according different scenarios. For a~~  
1339 ~~full description see Fig. 3~~

1340

1341 ~~Figure 5. Evapotranspiration estimated according different scenarios for the period~~  
1342 ~~June-August 2012. For a full description see Fig. 3.~~ ~~Figure 5. Evapotranspiration~~  
1343 ~~estimated according different scenarios for the period June August 2012. For a full~~  
1344 ~~description see Fig. 3.~~

1345

1346 ~~Figure 6. RMSE values of latent heat flux, sensible heat flux and soil heat flux for the~~  
1347 ~~period June-August 2012. For a description of the scenarios see section 3 of the~~  
1348 ~~paper.~~ ~~Figure 6. RMSE of latent heat flux for the period June August 2012. For a~~  
1349 ~~description of the scenarios see section 3 of the paper.~~

1350

1351 ~~Figure 7. RMSE of sensible heat flux for the period June August 2012. For a~~  
1352 ~~description of the scenarios see section 3 of the paper.~~

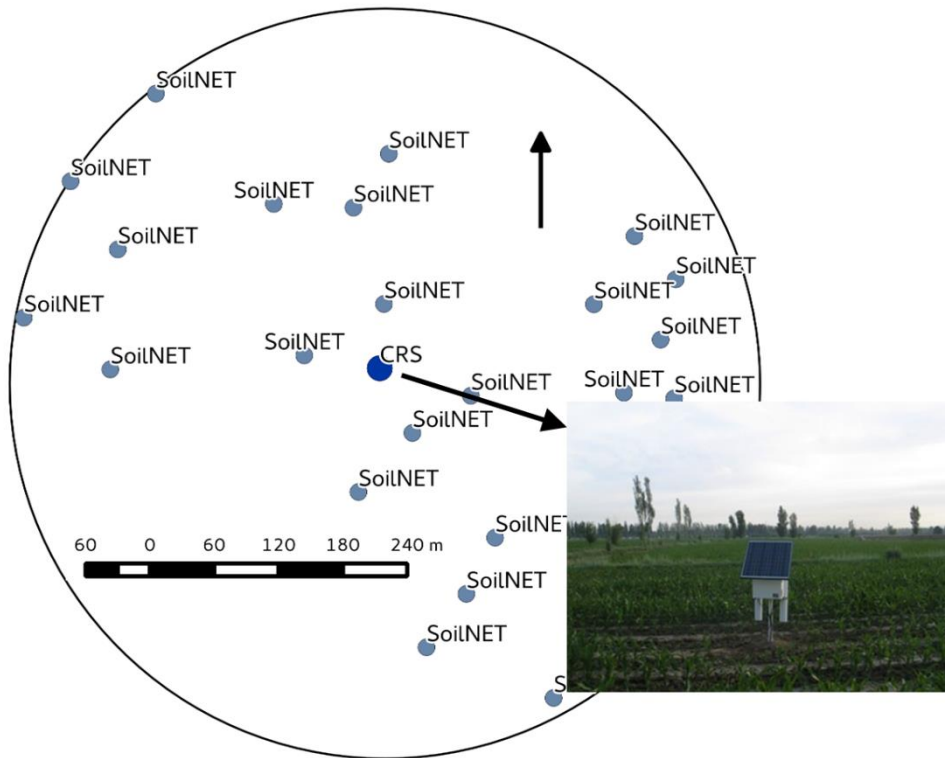
1353

1354 ~~Figure 8. RMSE of soil heat flux for the period June August 2012. For a description~~  
1355 ~~of the scenarios see section 3 of the paper.~~

1356

1357 Figure 97. ~~Leaf area index~~ LAI evolution for the period June-August 2012. Displayed  
1358 are the measured ~~leaf area index~~ LAI (Observation), default values (Background),  
1359 mean of ensemble members (Ens\_Mean) and ensemble members (Ensembles) for  
1360 scenarios of LST\_Feedback\_Par\_LAI (upper) and CRS\_LST\_Par\_LAI (lower)

1361



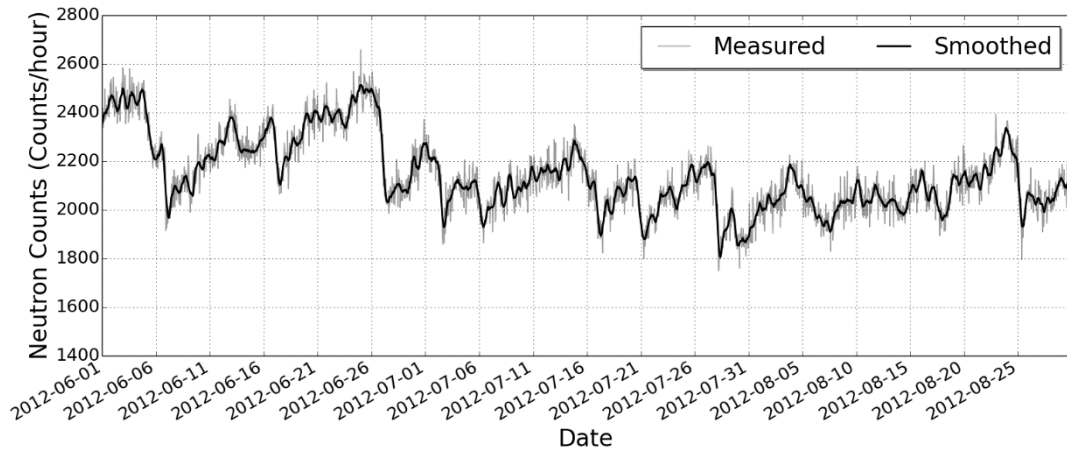
1362

1363

Figure 1. Map of the cosmic-ray probe and SoilNet Nodes in the footprint of the CRS probe positioned at the Heihe river catchment

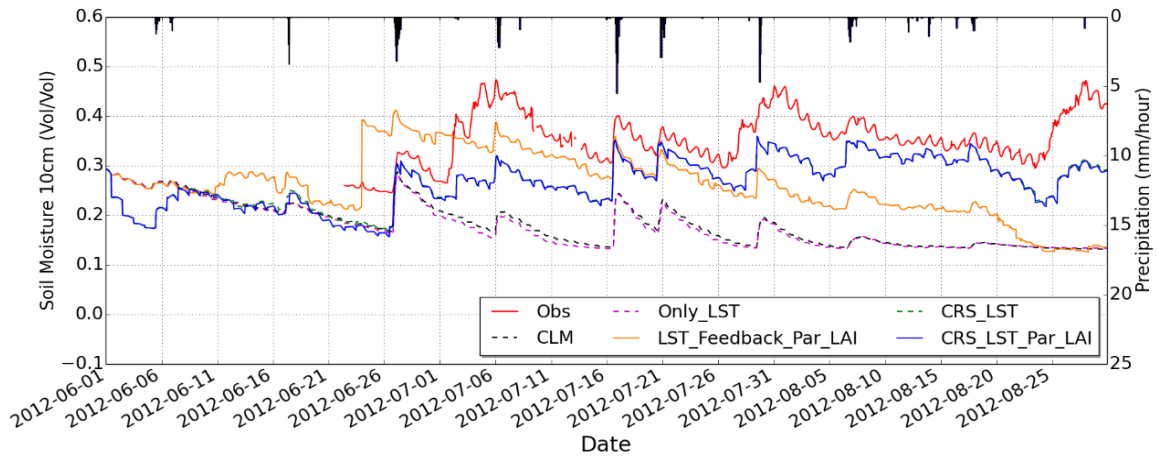
1364

1365

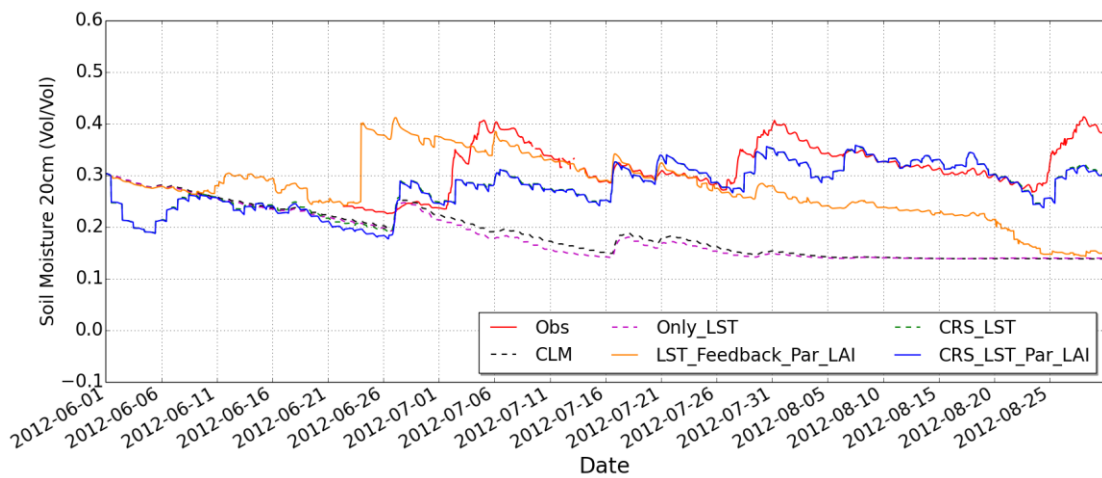


1366  
1367  
1368

Figure 2. Measured and temporally smoothed CRS neutron counts

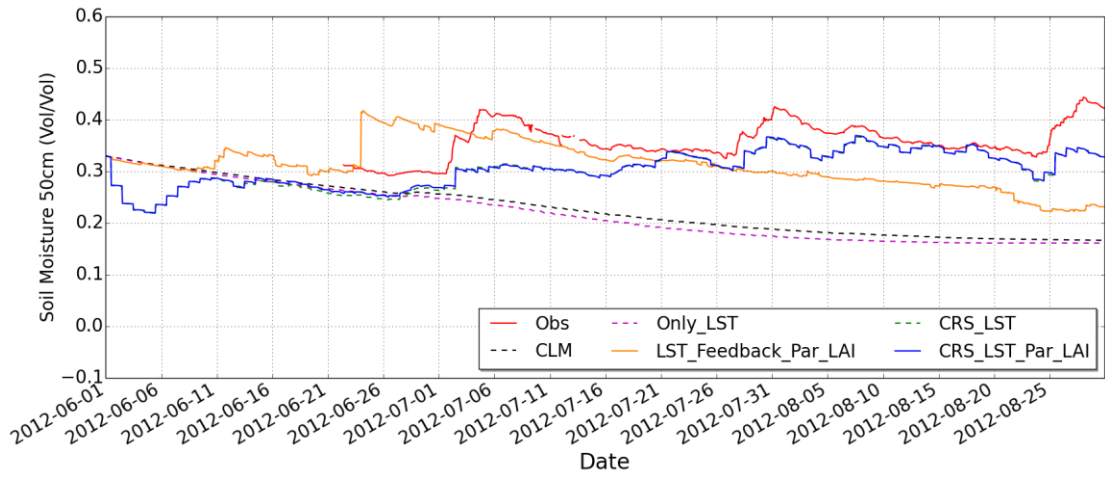


1369

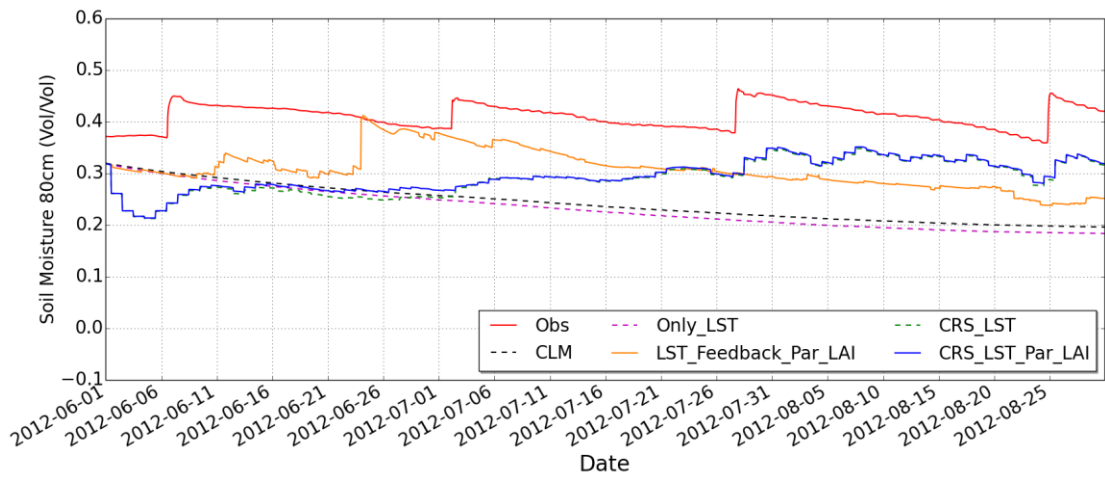


1370

1371 Figure 3. Soil moisture at 10 cm (upper) and 20 cm (lower) depth as obtained from an  
 1372 open loop run (CLM), local sensors (Obs), and different simulation scenarios. For a  
 1373 description of the scenarios see section 3 of the paper. The CRS neutron counts were  
 1374 assimilated from the 1<sup>st</sup> of June onwards.  
 1375



1376



1377

1378

1379

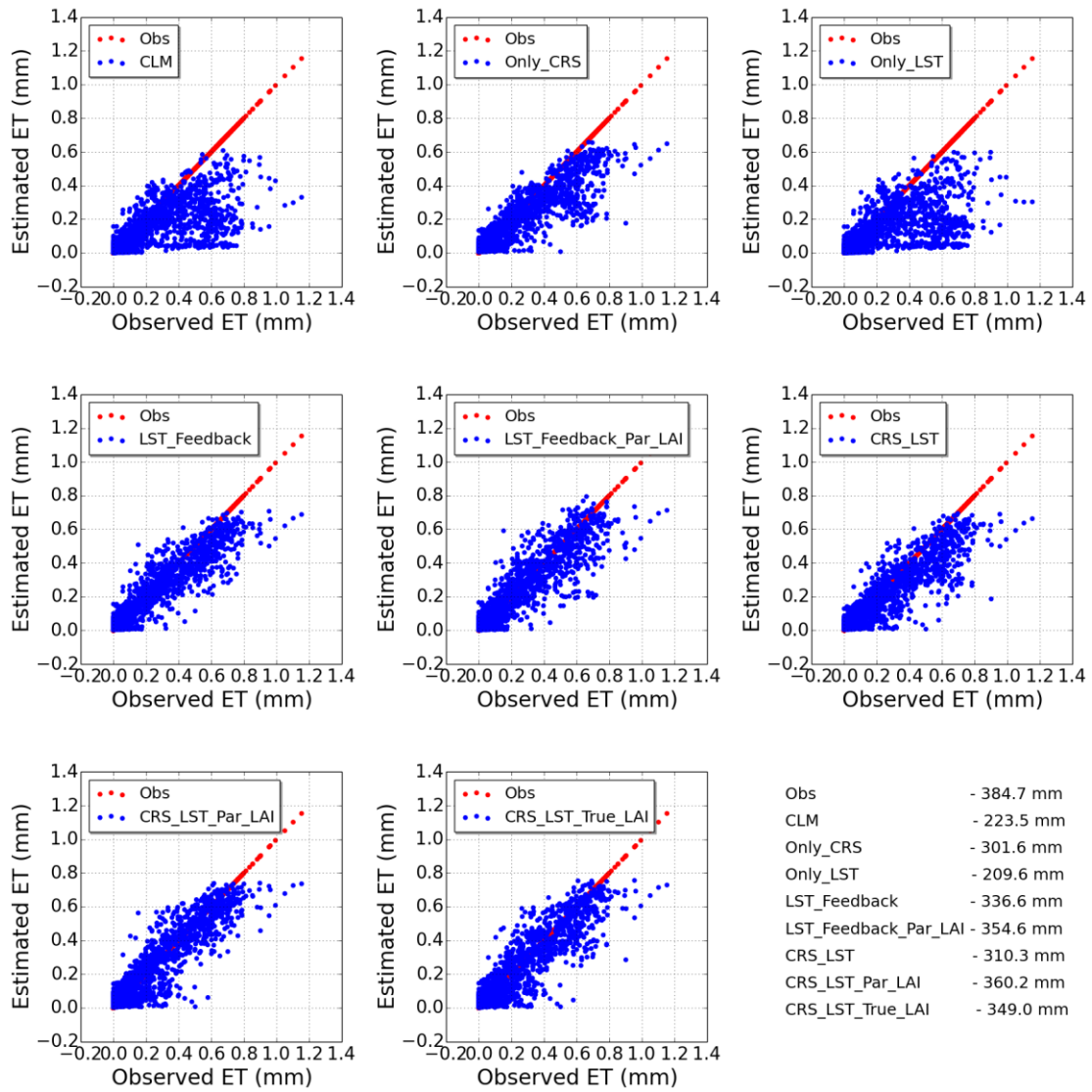
1380

1381

1382

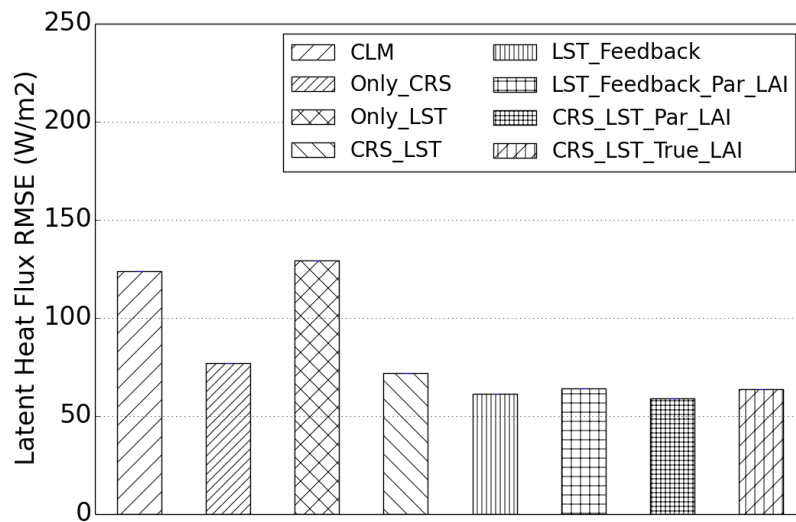
1383

Figure 4. Same as figure 3 but for 50 cm and 80 cm. Soil moisture at 50 (upper) cm- and 80 cm (lower) depth measured and modeled according different scenarios. For a full-description see Fig. 3.



1384  
 1385  
 1386  
 1387

Figure 5. Evapotranspiration estimated according different scenarios for the period June-August 2012. For a full description see Fig. 3.



1388  
 1389  
 1390  
 1391

Figure 6. RMSE of latent heat flux for the period June–August 2012. For a description of the scenarios see section 3 of the paper.



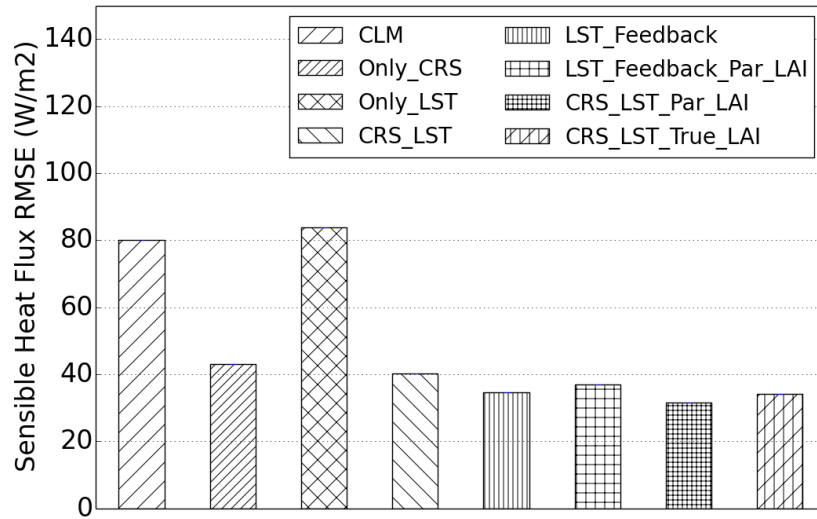
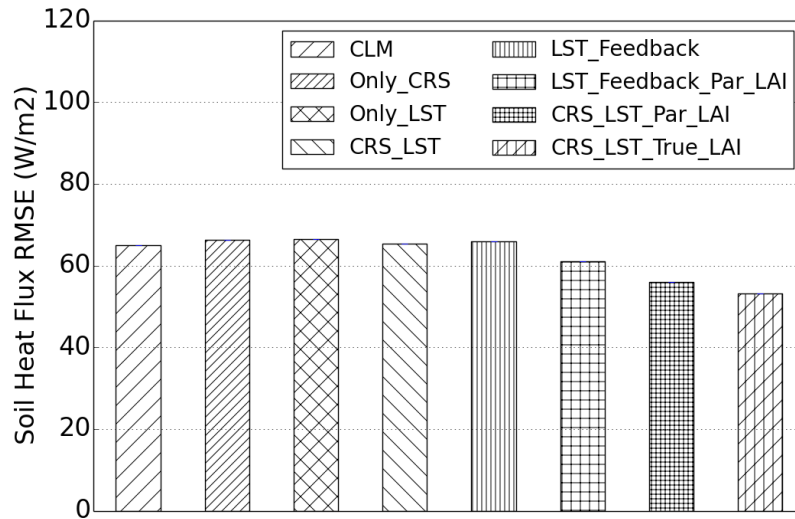


Figure 7. RMSE of sensible heat flux for the period June August 2012. For a description of the scenarios see section 3 of the paper.

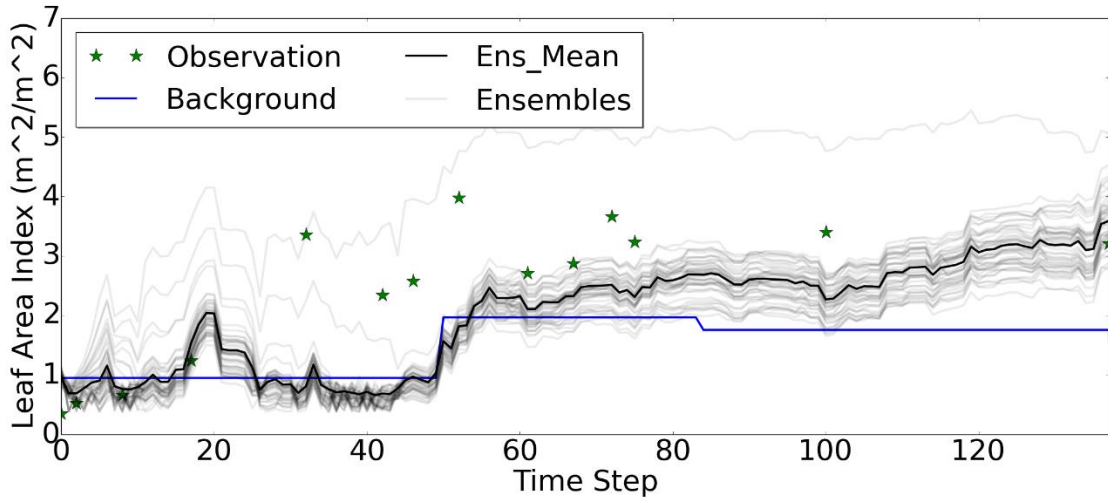
1392  
 1393  
 1394  
 1395



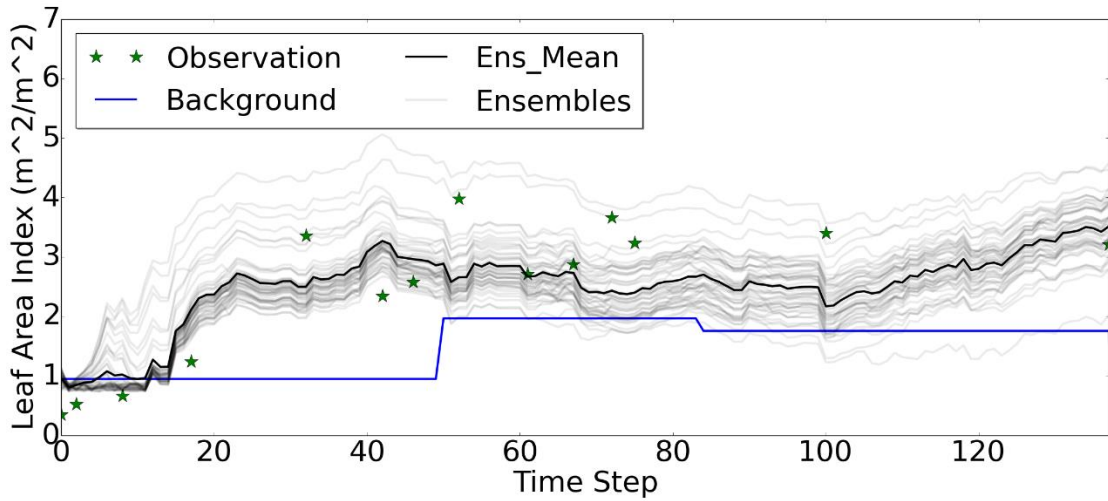
1396

1397 Figure 86. RMSE values of latent heat flux, sensible heat flux and soil heat flux for  
 1398 the period June-August 2012. For a description of the scenarios see section 3 of the  
 1399 paper.

1400



1401



1402

1403

1404

1405

1406

1407

1408

Figure 97. Leaf area index LAI evolution for the period June-August 2012. Displayed are the measured leaf area index LAI (Observation), default values (Background), mean of ensemble members (Ens\_Mean) and ensemble members (Ensembles) for scenarios of LST\_Feedback\_Par\_LAI (upper) and CRS\_LST\_Par\_LAI (lower)

1409 **References:**

- 1410 Anderson, M. C., Norman, J. M., Kustas, W. P., Li, F., Prueger, J. H., and Mecikalski, J. R.: Effects of  
1411 Vegetation Clumping on Two-Source Model Estimates of Surface Energy Fluxes from an Agricultural  
1412 Landscape during SMACEX, *J Hydrometeorol*, 6, 892-909, 2005.
- 1413 Barrett, D. J. and Renzullo, L. J.: On the Efficacy of Combining Thermal and Microwave Satellite Data as  
1414 Observational Constraints for Root-Zone Soil Moisture Estimation C-7972-2009, *J Hydrometeorol*, 10,  
1415 1109-1127, 2009.
- 1416 Bateni, S. M. and Entekhabi, D.: Surface heat flux estimation with the ensemble Kalman smoother:  
1417 Joint estimation of state and parameters, *Water Resour Res*, 48, 2012.
- 1418 Bogena, H. R., Herbst, M., Huisman, J. A., Rosenbaum, U., Weuthen, A., and Vereecken, H.: Potential of  
1419 Wireless Sensor Networks for Measuring Soil Water Content Variability, *Vadose Zone J*, 9, 1002-1013,  
1420 2010.
- 1421 Bogena, H. R., Huisman, J. A., Baatz, R., Hendricks Franssen, H. J., and Vereecken, H.: Accuracy of the  
1422 cosmic-ray soil water content probe in humid forest ecosystems: The worst case scenario, *Water*  
1423 *Resour Res*, 49, 5778-5791, 2013.
- 1424 Bosilovich, M. G., Radakovich, J. D., da Silva, A., Todling, R., and Verter, F.: Skin temperature analysis  
1425 and bias correction in a coupled land-atmosphere data assimilation system, *J Meteorol Soc Jpn*, 85A,  
1426 205-228, 2007.
- 1427 Collatz, G. J., Ball, J. T., Grivet, C., and Berry, J. A.: Physiological and Environmental-Regulation of  
1428 Stomatal Conductance, Photosynthesis and Transpiration - a Model That Includes a Laminar  
1429 Boundary-Layer, *Agr Forest Meteorol*, 54, 107-136, 1991.
- 1430 Crow, W. T., Kustas, W. P., and Prueger, J. H.: Monitoring root-zone soil moisture through the  
1431 assimilation of a thermal remote sensing-based soil moisture proxy into a water balance model,  
1432 *Remote Sens Environ*, 112, 1268-1281, 2008.
- 1433 Crow, W. T., van den Berg, M. J., Huffman, G. J., and Pellarin, T.: Correcting rainfall using satellite-based  
1434 surface soil moisture retrievals: The Soil Moisture Analysis Rainfall Tool (SMART), *Water Resour Res*, 47,  
1435 2011.
- 1436 Das, N. N., Mohanty, B. P., Cosh, M. H., and Jackson, T. J.: Modeling and assimilation of root zone soil  
1437 moisture using remote sensing observations in Walnut Gulch Watershed during SMEX04, *Remote Sens*  
1438 *Environ*, 112, 415-429, 2008.
- 1439 De Lannoy, G. J. M., Houser, P. R., Pauwels, V. R. N., and Verhoest, N. E. C.: State and bias estimation  
1440 for soil moisture profiles by an ensemble Kalman filter: Effect of assimilation depth and frequency,  
1441 *Water Resour Res*, 43, n/a-n/a, 2007.
- 1442 De Lannoy, G. J. M., Reichle, R. H., Arsenault, K. R., Houser, P. R., Kumar, S., Verhoest, N. E. C., and  
1443 Pauwels, V. R. N.: Multiscale assimilation of Advanced Microwave Scanning Radiometer-EOS snow  
1444 water equivalent and Moderate Resolution Imaging Spectroradiometer snow cover fraction  
1445 observations in northern Colorado, *Water Resour Res*, 48, 2012.
- 1446 Dee, D. P.: Bias and data assimilation, *Q J Roy Meteor Soc*, 131, 3323-3343, 2005.
- 1447 Desilets, D. and Zreda, M.: Footprint diameter for a cosmic-ray soil moisture probe: Theory and Monte  
1448 Carlo simulations, *Water Resour Res*, 49, 3566-3575, 2013.
- 1449 Desilets, D., Zreda, M., and Ferré, T. P. A.: Nature's neutron probe: Land surface hydrology at an elusive  
1450 scale with cosmic rays, *Water Resour. Res.*, 46, W11505, 2010.
- 1451 Draper, C. S., Mahfouf, J. F., and Walker, J. P.: Root zone soil moisture from the assimilation of  
1452 screen-level variables and remotely sensed soil moisture, *J Geophys Res-Atmos*, 116, 2011.

1453 Entekhabi, D., Njoku, E. G., O'Neill, P. E., Kellogg, K. H., Crow, W. T., Edelstein, W. N., Entin, J. K.,  
1454 Goodman, S. D., Jackson, T. J., Johnson, J., Kimball, J., Piepmeier, J. R., Koster, R. D., Martin, N.,  
1455 McDonald, K. C., Moghaddam, M., Moran, S., Reichle, R., Shi, J. C., Spencer, M. W., Thurman, S. W.,  
1456 Tsang, L., and Van Zyl, J.: The Soil Moisture Active Passive (SMAP) Mission, *IEEE Geoscience and Remote Sensing Letters*, 98, 704-716, 2010.

1457 Evensen, G.: The ensemble Kalman filter: Theoretical formulation and practical implementation,  
1458 *Ocean Dynam*, 53, 343-367, 2003.

1459 Franz, T. E., Zreda, M., Ferre, T. P. A., Rosolem, R., Zweck, C., Stillman, S., Zeng, X., and Shuttleworth, W.  
1460 J.: Measurement depth of the cosmic ray soil moisture probe affected by hydrogen from various  
1461 sources, *Water Resour Res*, 48, 2012.

1462 Franz, T. E., Zreda, M., Rosolem, R., and Ferre, T. P. A.: A universal calibration function for  
1463 determination of soil moisture with cosmic-ray neutrons, *Hydrology and Earth System Sciences*, 17,  
1464 453-460, 2013.

1465 Ghent, D., Kaduk, J., Remedios, J., Ardo, J., and Balzter, H.: Assimilation of land surface temperature  
1466 into the land surface model JULES with an ensemble Kalman filter, *J Geophys Res-Atmos*, 115, 2010.

1467 Ghilain, N., Arboleda, A., Sepulcre-Canto, G., Batelaan, O., Ardo, J., and Gellens-Meulenberghs, F.:  
1468 Improving evapotranspiration in a land surface model using biophysical variables derived from  
1469 MSG/SEVIRI satellite, *Hydrology and Earth System Sciences*, 16, 2567-2583, 2012.

1470 Han, X., Franssen, H.-J. H., Montzka, C., and Vereecken, H.: Soil moisture and soil properties estimation  
1471 in the Community Land Model with synthetic brightness temperature observations, *Water Resour Res*,  
1472 50, 6081-6105, 2014a.

1473 Han, X., Li, X., Franssen, H. J. H., Vereecken, H., and Montzka, C.: Spatial horizontal correlation  
1474 characteristics in the land data assimilation of soil moisture, *Hydrology and Earth System Sciences*, 16,  
1475 1349-1363, 2012.

1476 Han, X. J., Franssen, H. J. H., Li, X., Zhang, Y. L., Montzka, C., and Vereecken, H.: Joint Assimilation of  
1477 Surface Temperature and L-Band Microwave Brightness Temperature in Land Data Assimilation,  
1478 *Vadose Zone J*, 12, 0, 2013.

1479 Han, X. J., Hendricks Franssen, H. J., Jiménez Bello, M. A., Rosolem, R., Bogen, H., Martínez Alzamora,  
1480 F., Chanzy, A., and Vereecken, H.: Assimilation of cosmic-ray neutron counts for updating of soil  
1481 moisture and soil properties with  
1482 application to irrigation scheduling, *Journal of Hydrology*, submitted, 2014b.

1483 Han, X. J., Jin, R., Li, X., and Wang, S. G.: Soil Moisture Estimation Using Cosmic-Ray Soil Moisture  
1484 Sensing at Heterogeneous Farmland, *IEEE Geoscience and Remote Sensing Letters*, 11, 1659-1663,  
1485 2014c.

1486 Hunt, B. R., Kostelich, E. J., and Szunyogh, I.: Efficient data assimilation for spatiotemporal chaos: A  
1487 local ensemble transform Kalman filter, *Physica D: Nonlinear Phenomena*, 230, 112-126, 2007.

1488 Jarlan, L., Balsamo, G., Lafont, S., Beljaars, A., Calvet, J. C., and Mougin, E.: Analysis of leaf area index  
1489 in the ECMWF land surface model and impact on latent heat and carbon fluxes: Application to West  
1490 Africa, *J Geophys Res-Atmos*, 113, 2008.

1491 Jin, R., Li, X., Yan, B., Li, X., Luo, W., Ma, M., Guo, J., Kang, J., Zhu, Z., and Zhao, S.: A Nested  
1492 Ecohydrological Wireless Sensor Network for Capturing the Surface Heterogeneity in the Midstream  
1493 Areas of the Heihe River Basin, China, *IEEE Geoscience and Remote Sensing Letters*, PP, 1-5, 2014.

1494 Jin, R., Wang, X., Kang, J., Wang, Z., Dong, C., and Li, D.: HiWATER: SoilNET observation dataset in the  
1495 middle reaches of the Heihe river basin, Heihe Plan Science Data Center, doi:  
1496 10.3972/hiwater.120.2013.db

1497 doi:10.3972/hiwater.120.2013.db, 2013. 2013.

1498 Kerr, Y. H., Waldteufel, P., Wigneron, J. P., Delwart, S., Cabot, F., Boutin, J., Escorihuela, M. J., Font, J.,  
1499 Reul, N., Gruhier, C., and Others: The SMOS Mission: New Tool for Monitoring Key Elements of the  
1500 Global Water Cycle, *IEEE*, 98, 666–687, 2010.

1501 Kumar, S. V., Reichle, R. H., Harrison, K. W., Peters-Lidard, C. D., Yatheendradas, S., and Santanello, J. A.:  
1502 A comparison of methods for a priori bias correction in soil moisture data assimilation, *Water Resour*  
1503 *Res*, 48, n/a-n/a, 2012.

1504 Kumar, S. V., Reichle, R. H., Koster, R. D., Crow, W. T., and Peters-Lidard, C. D.: Role of Subsurface  
1505 Physics in the Assimilation of Surface Soil Moisture Observations, *J Hydrometeorol*, 10, 1534-1547,  
1506 2009.

1507 Kustas, W. and Anderson, M.: Advances in thermal infrared remote sensing for land surface modeling,  
1508 *Agr Forest Meteorol*, 149, 2071-2081, 2009.

1509 Li, C. and Ren, L.: Estimation of Unsaturated Soil Hydraulic Parameters Using the Ensemble Kalman  
1510 Filter, *Vadose Zone J*, 10, 1205, 2011.

1511 Li, F. Q., Crow, W. T., and Kustas, W. P.: Towards the estimation root-zone soil moisture via the  
1512 simultaneous assimilation of thermal and microwave soil moisture retrievals, *Adv Water Resour*, 33,  
1513 201-214, 2010.

1514 Li, X., Cheng, G. D., Liu, S. M., Xiao, Q., Ma, M. G., Jin, R., Che, T., Liu, Q. H., Wang, W. Z., Qi, Y., Wen, J.  
1515 G., Li, H. Y., Zhu, G. F., Guo, J. W., Ran, Y. H., Wang, S. G., Zhu, Z. L., Zhou, J., Hu, X. L., and Xu, Z. W.:  
1516 Heihe Watershed Allied Telemetry Experimental Research (HiWATER): Scientific Objectives and  
1517 Experimental Design, *B Am Meteorol Soc*, 94, 1145-1160, 2013.

1518 Miyoshi, T. and Yamane, S.: Local Ensemble Transform Kalman Filtering with an AGCM at a T159/L48  
1519 Resolution, *Mon Weather Rev*, 135, 3841-3861, 2007.

1520 Montzka, C., Grant, J. P., Moradkhani, H., Franssen, H. J. H., Weihermuller, L., Drusch, M., and  
1521 Vereecken, H.: Estimation of Radiative Transfer Parameters from L-Band Passive Microwave Brightness  
1522 Temperatures Using Advanced Data Assimilation, *Vadose Zone J*, 12, 2013.

1523 Moradkhani, H., Sorooshian, S., Gupta, H. V., and Houser, P. R.: Dual state–parameter estimation of  
1524 hydrological models using ensemble Kalman filter, *Adv Water Resour*, 28, 135-147, 2005.

1525 Nie, S., Zhu, J., and Luo, Y.: Simultaneous estimation of land surface scheme states and parameters  
1526 using the ensemble Kalman filter: identical twin experiments, *Hydrology and Earth System Sciences*,  
1527 15, 2437-2457, 2011.

1528 Oleson, K., Lawrence, D. M., Bonan, G., Drewniak, B., Huang, M., Koven, C. D., Levis, S., Li, F., Riley, W.  
1529 J., Subin, Z. M., Swenson, S. C., Thornton, P. E., Bozbiyik, A., Fisher, B. E. A., Kluzek, E., Lamarque, J. F.,  
1530 Lawrence, P. J., Leung, L. R., Lipscomb, W., Muszala, S., Ricciuto, D. M., Sacks, W., Sun, Y., Tang, J., and  
1531 Yang, Z.-L.: Technical Description of version 4.5 of the Community Land Model (CLM), *Ncar Technical*  
1532 *Note NCAR/TN-503+STR*, National Center for Atmospheric Research, Boulder, CO, 422 pp., 2013. 2013.

1533 Pauwels, V. R. N., Balenzano, A., Satalino, G., Skriver, H., Verhoest, N. E. C., and Mattia, F.: Optimization  
1534 of Soil Hydraulic Model Parameters Using Synthetic Aperture Radar Data: An Integrated  
1535 Multidisciplinary Approach, *IEEE T Geosci Remote*, 47, 455-467, 2009.

1536 Reichle, R. H.: Data assimilation methods in the Earth sciences, *Adv Water Resour*, 31, 1411-1418,  
1537 2008.

1538 Reichle, R. H., Kumar, S. V., Mahanama, S. P. P., Koster, R. D., and Liu, Q.: Assimilation of  
1539 Satellite-Derived Skin Temperature Observations into Land Surface Models, *J Hydrometeorol*, 11,  
1540 1103-1122, 2010.

1541 Robinson, D. A., Jones, S. B., Wraith, J. M., Or, D., and Friedman, S. P.: A Review of Advances in  
1542 Dielectric and Electrical Conductivity Measurement in Soils Using Time Domain Reflectometry, *Vadose*  
1543 *Zone J.*, 2, 444-475, 2003.

1544 Rodell, M., Houser, P. R., Jambor, U., Gottschalck, J., Mitchell, K., Meng, C. J., Arsenault, K., Cosgrove,  
1545 B., Radakovich, J., Bosilovich, M., Entin, J. K., Walker, J. P., Lohmann, D., and Toll, D.: The global land  
1546 data assimilation system, *B Am Meteorol Soc*, 85, 381-+, 2004.

1547 Rosolem, R., Hoar, T., Arellano, a., Anderson, J. L., Shuttleworth, W. J., Zeng, X., and Franz, T. E.:  
1548 Assimilation of near-surface cosmic-ray neutrons improves summertime soil moisture profile  
1549 estimates at three distinct biomes in the USA, *Hydrology and Earth System Sciences*, submitted,  
1550 2014a.

1551 Rosolem, R., Hoar, T., Arellano, A., Anderson, J. L., Shuttleworth, W. J., Zeng, X., and Franz, T. E.:  
1552 Assimilation of near-surface cosmic-ray neutrons improves summertime soil moisture profile  
1553 estimates at three distinct biomes in the USA, *Hydrol. Earth Syst. Sci. Discuss.*, 11, 5515-5558, 2014b.

1554 Rosolem, R., Shuttleworth, W. J., Zreda, M., Franz, T. E., Zeng, X., and Kurc, S. A.: The Effect of  
1555 Atmospheric Water Vapor on Neutron Count in the Cosmic-Ray Soil Moisture Observing System, *J*  
1556 *Hydrometeorol*, 14, 1659-1671, 2013.

1557 Savitzky, A. and Golay, M. J. E.: Smoothing and Differentiation of Data by Simplified Least Squares  
1558 Procedures, *Analytical Chemistry*, 36, 1627-1639, 1964.

1559 Schwinger, J., Kollet, S. J., Hoppe, C. M., and Elbern, H.: Sensitivity of Latent Heat Fluxes to Initial  
1560 Values and Parameters of a Land-Surface Model, *Vadose Zone J*, 9, 984-1001, 2010.

1561 Shangguan, W., Dai, Y., Liu, B., Zhu, A., Duan, Q., Wu, L., Ji, D., Ye, A., Yuan, H., Zhang, Q., Chen, D.,  
1562 Chen, M., Chu, J., Dou, Y., Guo, J., Li, H., Li, J., Liang, L., Liang, X., Liu, H., Liu, S., Miao, C., and Zhang, Y.:  
1563 A China data set of soil properties for land surface modeling, *J Adv Model Earth Sy*, 5, 212-224, 2013.

1564 Shuttleworth, J., Rosolem, R., Zreda, M., and Franz, T. E.: The COsmic-ray Soil Moisture Interaction  
1565 Code (COSMIC) for use in data assimilation, *Hydrology and Earth System Sciences*, 17, 3205-3217,  
1566 2013.

1567 Sun, W. X., Liang, S. L., Xu, G., Fang, H. L., and Dickinson, R.: Mapping plant functional types from  
1568 MODIS data using multisource evidential reasoning, *Remote Sens Environ*, 112, 1010-1024, 2008.

1569 van den Hurk, B. J. J. M.: Impact of leaf area index seasonality on the annual land surface evaporation  
1570 in a global circulation model, *Journal of Geophysical Research*, 108, 2003.

1571 Wan, Z. and Li, Z. L.: Radiance - based validation of the V5 MODIS land - surface temperature product,  
1572 *Int J Remote Sens*, 29, 5373-5395, 2008.

1573 Xu, T. R., Liang, S. L., and Liu, S. M.: Estimating turbulent fluxes through assimilation of geostationary  
1574 operational environmental satellites data using ensemble Kalman filter, *J Geophys Res-Atmos*, 116,  
1575 2011.

1576 Xu, Z. W., Liu, S. M., Li, X., Shi, S. J., Wang, J. M., Zhu, Z. L., Xu, T. R., Wang, W. Z., and Ma, M. G.:  
1577 Intercomparison of surface energy flux measurement systems used during the HiWATER-MUSOEXE, *J*  
1578 *Geophys Res-Atmos*, 118, 13140-13157, 2013.

1579 Yang, K., Koike, T., Kaihotsu, I., and Qin, J.: Validation of a Dual-Pass Microwave Land Data Assimilation  
1580 System for Estimating Surface Soil Moisture in Semiarid Regions, *J Hydrometeorol*, 10, 780-793, 2009.

1581 Yang, Z. L., Dai, Y., Dickinson, R. E., and Shuttleworth, W. J.: Sensitivity of ground heat flux to  
1582 vegetation cover fraction and leaf area index, *J Geophys Res-Atmos*, 104, 19505-19514, 1999.

1583 Zhu, C. Y., Byrd, R. H., Lu, P. H., and Nocedal, J.: Algorithm 778: L-BFGS-B: Fortran subroutines for  
1584 large-scale bound-constrained optimization, *Acm Transactions on Mathematical Software*, 23, 550-560,

1585 1997.  
1586 Zreda, M., Desilets, D., Ferre, T. P. A., and Scott, R. L.: Measuring soil moisture content non-invasively  
1587 at intermediate spatial scale using cosmic-ray neutrons, *Geophys Res Lett*, 35, L21402, 2008.  
1588 Zreda, M., Shuttleworth, W. J., Zeng, X., Zweck, C., Desilets, D., Franz, T. E., and Rosolem, R.: COSMOS:  
1589 the COsmic-ray Soil Moisture Observing System, *Hydrology and Earth System Sciences*, 16, 4079-4099,  
1590 2012.  
1591